reactivation in patients with B-cell non-Hodgkin lymphoma following rituximab containing chemotherapy: results of interim analysis. *Blood* 2012; **120**: 2641.

313 Mochida T. Health and Science Research Grant from Ministry of Health, Labour and Welfare. Research on Hepatitis. HBV Reactivation through immunosuppressive and/or anti-cancer therapies, elucidation and establishment of countermeasures. 2011 report by the "HBV Reactivation through Immunosuppressive and/or Anti-cancer Therapies" Research Group, 2012. (In Japanese.)

314 Japan College of Rheumatology. A proposal for management of rheumatic disease patients with hepatitis B virus infection receiving immunosuppressive therapy. 2011. (In Japanese.)

315 Berger A, Preiser W, Kachel HG *et al.* HBV reactivation after kidney transplantation. *J Clin Virol* 2005; **32**: 162–5.

316 Hui CK, Cheung WW, Zhang HY *et al.* Kinetics and risk of de novo hepatitis B infection in HBsAg-negative patients undergoing cytotoxic chemotherapy. *Gastroenterology* 2006; **131**: 59–68.

317 Westhoff TH, Jochimsen F, Schmittel A *et al.* Fatal hepatitis B virus reactivation by an escape mutant following rituximab therapy. *Blood* 2003; **102**: 1930.

318 Cheng J, Li JB, Sun QL *et al.* Reactivation of hepatitis B virus after steroid treatment in rheumatic diseases. *J Rheumatol* 2011; **38**: 181–2.

319 Narvaez J, Rodriguez-Moreno J, Martinez-Aguila MD *et al.* Severe hepatitis linked to B virus infection after withdrawal of low dose methotrexate therapy. *J Rheumatol* 1998; **25**: 2037–8.

320 Hagiyama H, Kubota T, Komano Y *et al.* Fulminant hepatitis in an asymptomatic chronic carrier of hepatitis B virus mutant after withdrawal of low-dose methotrexate therapy for rheumatoid arthritis. *Clin Exp Rheumatol* 2004; **22**: 375–6.

321 Ito S, Nakazono K, Murasawa A *et al.* Development of fulminant hepatitis B (precore variant mutant type) after the discontinuation of low-dose methotrexate therapy in a rheumatoid arthritis patient. *Arthritis Rheum* 2001; **44**: 339–42.

322 Chen CH, Chen PJ, Chu JS *et al.* Fibrosing cholestatic hepatitis in a hepatitis B surface antigen carrier after renal transplantation. *Gastroenterology* 1994; **107**: 1514–18.

323 McIvor C, Morton J, Bryant A *et al.* Fatal reactivation of precore mutant hepatitis B virus associated with fibrosing cholestatic hepatitis after bone marrow transplantation. *Ann Intern Med* 1994; **121**: 274–5.

324 Vassilopoulos D, Calabrese LH. Risks of immunosuppressive therapies including biologic agents in patients with rheumatic diseases and co-existing chronic viral infections. *Curr Opin Rheumatol* 2007; **19**: 619–25.

325 Yeo W, Chan PK, Ho WM *et al.* Lamivudine for the prevention of hepatitis B virus reactivation in hepatitis B s-antigen seropositive cancer patients undergoing cytotoxic chemotherapy. *J Clin Oncol* 2004; **22**: 927–34.

326 Hsu C, Hsiung CA, Su IJ *et al.* A revisit of prophylactic lamivudine for chemotherapy-associated hepatitis B reactivation in non-Hodgkin's lymphoma: a randomized trial. *Hepatology* 2008; **47**: 844–53.

327 Lau GK, He ML, Fong DY *et al.* Preemptive use of lamivudine reduces hepatitis B exacerbation after allogeneic hematopoietic cell transplantation. *Hepatology* 2002; **36**: 702–9.

328 Loomba R, Rowley A, Wesley R *et al.* Systematic review: the effect of preventive lamivudine on hepatitis B reactivation during chemotherapy. *Ann Intern Med* 2008; **148**: 519–28.

329 Watanabe M, Shibuya A, Takada J *et al.* Entecavir is an optional agent to prevent hepatitis B virus (HBV) reactivation: a review of 16 patients. *Eur J Intern Med* 2010; **21**: 333–7.

330 Jimenez-Perez M, Saez-Gomez AB, Mongil Poce L *et al.* Efficacy and safety of entecavir and/or tenofovir for prophylaxis and treatment of hepatitis B recurrence post-liver transplant. *Transplant Proc* 2010; **42**: 3167–8.

331 Tamori A, Koike T, Goto H *et al.* Prospective study of reactivation of hepatitis B virus in patients with rheumatoid arthritis who received immunosuppressive therapy: evaluation of both HBsAg-positive and HBsAg-negative cohorts. *J Gastroenterol* 2011; **46**: 556–64.

332 Uemoto S, Sugiyama K, Marusawa H *et al.* Transmission of hepatitis B virus from hepatitis B core antibody-positive donors in living related liver transplants. *Transplantation* 1998; **65**: 494–9.

333 Terrault N. Management of hepatitis B virus infection in liver transplant recipients: prospects and challenges. *Clin Transplant* 2000; **14** (Suppl 2): 39–43.

334 Markowitz JS, Martin P, Conrad AJ *et al.* Prophylaxis against hepatitis B recurrence following liver transplantation using combination lamivudine and hepatitis B immune globulin. *Hepatology* 1998; **28**: 585–9.

335 Umeda M, Marusawa H, Ueda M *et al.* Beneficial effects of short-term lamivudine treatment for de novo hepatitis B virus reactivation after liver transplantation. *Am J Transplant* 2006; **6**: 2680–5.

336 Marcellin P, Giostra E, Martinot-Peignoux M *et al.* Redevelopment of hepatitis B surface antigen after renal transplantation. *Gastroenterology* 1991; **100**: 1432–4.

337 Dusheiko G, Song E, Bowyer S *et al.* Natural history of hepatitis B virus infection in renal transplant recipients-a fifteen-year follow-up. *Hepatology* 1983; **3**: 330–6.

338 Degos F, Lugassy C, Degott C *et al.* Hepatitis B virus and hepatitis B-related viral infection in renal transplant recipients. A prospective study of 90 patients. *Gastroenterology* 1988; **94**: 151–6.

339 Park SK, Yang WS, Lee YS *et al.* Outcome of renal transplantation in hepatitis B surface antigen-positive patients after introduction of lamivudine. *Nephrol Dial Transplant* 2001; **16**: 2222–8.

340 Lau GK, Liang R, Chiu EK *et al.* Hepatic events after bone marrow transplantation in patients with hepatitis B infection: a case controlled study. *Bone Marrow Transplant* 1997; **19**: 795–9.
341 Dhedin N, Douvin C, Kuentz M *et al.* Reverse seroconversion of hepatitis B after allogeneic bone marrow transplantation: a retrospective study of 37 patients with pretransplant anti-HBs and anti-HBc. *Transplantation* 1998; **66**: 616–19.
342 Seth P, Alrajhi AA, Kagevi I *et al.* Hepatitis B virus reactivation with clinical flare in allogeneic stem cell transplants with chronic graft-versus-host disease. *Bone Marrow Transplant* 2002; **30**: 189–94.
343 Matsue K, Aoki T, Odawara J *et al.* High risk of hepatitis B-virus reactivation after hematopoietic cell transplantation in hepatitis B core antibody-positive patients. *Eur J Haematol* 2009; **83**: 357–64.
344 Oshima K, Sato M, Okuda S *et al.* Reverse seroconversion of hepatitis B virus after allogeneic hematopoietic stem cell transplantation in the absence of chronic graft-versus-host disease. *Hematology* 2009; **14**: 73–5.
345 Yeo W, Chan PK, Zhong S *et al.* Frequency of hepatitis B virus reactivation in cancer patients undergoing cytotoxic chemotherapy: a prospective study of 626 patients with identification of risk factors. *J Med Virol* 2000; **62**: 299–307.
346 Yeo W, Chan TC, Leung NW *et al.* Hepatitis B virus reactivation in lymphoma patients with prior resolved hepatitis B undergoing anticancer therapy with or without rituximab. *J Clin Oncol* 2009; **27**: 605–11.
347 Hsu C, Tsou H, Lin S *et al.* Incidence of hepatitis B (HBV) reactivation in non-Hodgkins lymphoma patients with resolved HBV infection and received rituximab-containing chemotherapy. *Hepatol Int* 2012; **6**: 65.
348 Umemura T, Tanaka E, Kiyosawa K *et al.* Mortality secondary to fulminant hepatic failure in patients with prior resolution of hepatitis B virus infection in Japan. *Clin Infect Dis* 2008; **47**: e52–6.
349 Lau GK, Yiu HH, Fong DY *et al.* Early is superior to deferred preemptive lamivudine therapy for hepatitis B patients undergoing chemotherapy. *Gastroenterology* 2003; **125**: 1742–9.
350 Lok AS, Liang RH, Chiu EK *et al.* Reactivation of hepatitis B virus replication in patients receiving cytotoxic therapy. Report of a prospective study. *Gastroenterology* 1991; **100**: 182–8.
351 Nakamura Y, Motokura T, Fujita A *et al.* Severe hepatitis related to chemotherapy in hepatitis B virus carriers with hematologic malignancies. Survey in Japan, 1987–1991. *Cancer* 1996; **78**: 2210–15.
352 Yeo W, Zee B, Zhong S *et al.* Comprehensive analysis of risk factors associating with Hepatitis B virus (HBV) reactivation in cancer patients undergoing cytotoxic chemotherapy. *Br J Cancer* 2004; **90**: 1306–11.
353 Calabrese LH, Zein NN, Vassilopoulos D. Hepatitis B virus (HBV) reactivation with immunosuppressive therapy in rheumatic diseases: assessment and preventive strategies. *Ann Rheum Dis* 2006; **65**: 983–9.
354 Tanaka E, Urata Y. Risk of hepatitis B reactivation in patients treated with tumor necrosis factor-alpha inhibitors. *Hepatol Res* 2012; **42**: 333–9.
355 Iannitto E, Minardi V, Calvaruso G *et al.* Hepatitis B virus reactivation and alemtuzumab therapy. *Eur J Haematol* 2005; **74**: 254–8.
356 Ritchie D, Piekarz RL, Blombery P *et al.* Reactivation of DNA viruses in association with histone deacetylase inhibitor therapy: a case series report. *Haematologica* 2009; **94**: 1618–22.
357 Tanaka H, Sakuma I, Hashimoto S *et al.* Hepatitis B reactivation in a multiple myeloma patient with resolved hepatitis B infection during bortezomib therapy: case report. *J Clin Exp Hematop* 2012; **52**: 67–9.
358 Koike K, Kikuchi Y, Kato M *et al.* Prevalence of hepatitis B virus infection in Japanese patients with HIV. *Hepatol Res* 2008; **38**: 310–14.
359 Nishida K, Yamamoto Y, Kagawa K *et al.* The prevalence of co-infection with hepatitis viruses in human immunodeficiency virus (HIV) infected patients in Japan and the efficacy of hepatitis B virus (HBV)/hepatitis A virus (HAV) vaccination. *J Aids Res* 2007; **9**: 30–5. (In Japanese.)
360 Bodsworth NJ, Cooper DA, Donovan B. The influence of human immunodeficiency virus type 1 infection on the development of the hepatitis B virus carrier state. *J Infect Dis* 1991; **163**: 1138–40.
361 Koibuchi T, Hitani A, Nakamura T *et al.* Predominance of genotype A HBV in an HBV-HIV-1 dually positive population compared with an HIV-1-negative counterpart in Japan. *J Med Virol* 2001; **64**: 435–40.
362 Nunez M. Hepatotoxicity of antiretrovirals: incidence, mechanisms and management. *J Hepatol* 2006; **44**: S132–9.
363 de Vries-Sluijs TE, Reijnders JG, Hansen BE *et al.* Long-term therapy with tenofovir is effective for patients co-infected with human immunodeficiency virus and hepatitis B virus. *Gastroenterology* 2010; **139**: 1934–41.
364 Wever K, van Agtmael MA, Carr A. Incomplete reversibility of tenofovir-related renal toxicity in HIV-infected men. *J Acquir Immune Defic Syndr* 2010; **55**: 78–81.
365 Guidelines for the Use of Antiretroviral Agents in HIV-1-Infected Adults and Adolescents. 2012. Developed by the HHS Panel on Antiretroviral Guidelines for Adults and Adolescents – A Working Group of the Office of AIDS Research Advisory Council (OARAC). (http://aidsinfo.nih.gov/guidelines) 2013.
366 Koibuchi T, Shirosaka T *et al.* Health and Science Research Grant from Ministry of Health, Labour and Welfare. Research on AIDS Control Measures. Guidelines for anti-HIV therapy. HIV Infection and Complications Research Group, 2012. (In Japanese.)

OPEN ACCESS Freely available online

PLOS ONE

Inhibitory Effects of Caffeic Acid Phenethyl Ester Derivatives on Replication of Hepatitis C Virus

Hui Shen[1], Atsuya Yamashita[1], Masamichi Nakakoshi[2], Hiromasa Yokoe[3], Masashi Sudo[3], Hirotake Kasai[1], Tomohisa Tanaka[1], Yuusuke Fujimoto[1], Masanori Ikeda[4], Nobuyuki Kato[4], Naoya Sakamoto[5], Hiroko Shindo[6], Shinya Maekawa[6], Nobuyuki Enomoto[6], Masayoshi Tsubuki[3]*, Kohji Moriishi[1]*

1 Department of Microbiology, Division of Medicine, Graduate School of Medicine and Engineering, University of Yamanashi, Yamanashi, Japan, **2** Faculty of Pharmaceutical Sciences, Toho University, Chiba, Japan, **3** Institute of Medical Chemistry, Hoshi University, Tokyo, Japan, **4** Department of Tumor Virology, Okayama University Graduate School of Medicine, Dentistry, and Pharmaceutical Sciences, Okayama, Japan, **5** Department of Gastroenterology and Hepatology, Hokkaido University Graduate School of Medicine, Sapporo, Japan, **6** First Department of Internal Medicine, Faculty of Medicine, University of Yamanashi, Yamanashi, Japan

Abstract

Caffeic acid phenethyl ester (CAPE) has been reported as a multifunctional compound. In this report, we tested the effect of CAPE and its derivatives on hepatitis C virus (HCV) replication in order to develop an effective anti-HCV compound. CAPE and CAPE derivatives exhibited anti-HCV activity against an HCV replicon cell line of genotype 1b with EC_{50} values in a range from 1.0 to 109.6 μM. Analyses of chemical structure and antiviral activity suggested that the length of the n-alkyl side chain and catechol moiety are responsible for the anti-HCV activity of these compounds. Caffeic acid n-octyl ester exhibited the highest anti-HCV activity among the tested derivatives with an EC_{50} value of 1.0 μM and an SI value of 63.1 by using the replicon cell line derived from genotype 1b strain Con1. Treatment with caffeic acid n-octyl ester inhibited HCV replication of genotype 2a at a similar level to that of genotype 1b irrespectively of interferon signaling. Caffeic acid n-octyl ester could synergistically enhance the anti-HCV activities of interferon-alpha 2b, daclatasvir, and VX-222, but neither telaprevir nor danoprevir. These results suggest that caffeic acid n-octyl ester is a potential candidate for novel anti-HCV chemotherapy drugs.

Citation: Shen H, Yamashita A, Nakakoshi M, Yokoe H, Sudo M, et al. (2013) Inhibitory Effects of Caffeic Acid Phenethyl Ester Derivatives on Replication of Hepatitis C Virus. PLoS ONE 8(12): e82299. doi:10.1371/journal.pone.0082299

Editor: Hak Hotta, Kobe University, Japan

Received September 15, 2013; **Accepted** October 31, 2013; **Published** December 17, 2013

Funding: This work was supported in part by grants-in-aid from the Ministry of Health, Labor, and Welfare and from the Ministry of Education, Culture, Sports, Science, and Technology of Japan. The funders had no role in study design, data collection and analysis, decision to publish, or preparation of the manuscript.

Competing Interests: The authors have declared that no competing interests exist.

* E-mail: tsubuki@hoshi.ac.jp (MT); kmoriishi@yamanashi.ac.jp (KM)

Introduction

Hepatitis C virus (HCV) is well known as a major causative agent of chronic liver disease including cirrhosis and hepatocellular carcinoma and is thought to persistently infect 170 million patients worldwide [1]. HCV belongs to the genus *Hepacivirus* of the family *Flaviviridae* and possesses a viral genome that is characterized by a single positive strand RNA with a nucleotide length of 9.6 kb [2]. The single polypeptide coded by the genome is composed of 3,000 amino acids and is cleaved by host and viral proteases, resulting in 10 proteins, which are classified into structural and nonstructural proteins [3]. The viral genome is transcribed by a replication complex consisting of NS3 to NS5B and host factors [4]. NS3 forms a complex with NS4A and becomes a fully active form to cleave the C-terminal parts of the nonstructural proteins. The advanced NS3/4A protease inhibitors, telaprevir and boceprevir, have been employed in the treatment of chronic hepatitis C patients infected with genotype 1 [5]. Sustained virologic response (SVR) was reportedly 80% in patients infected with genotype 1 following triple combination therapy with pegylated interferon, ribavirin, and telaprevir [6], although the therapy exhibits side effects including rash, severe cutaneous eruption, influenza-like symptoms, cytopenias, depression, and anemia [7]. In addition, there is the possibility of the emergence of drug-resistant viruses following treatment with those anti-HCV drugs [8] Thus, further study is required for development of safer and more effective anti-HCV compounds.

Several recent reports indicate that silbinin [9], epigallocatechin-3-gallate [10], curcumin [11], quercetin [12] and proanthocyanidins [13], which all originate from natural sources, have exhibited inhibitory activity against HCV replication in cultured cells. Caffeic acid phenethyl ester (CAPE) is an active component included in propolis prepared from honeybee hives, and has a similar structure to flavonoids (Fig. 1A). CAPE has multifunctional properties containing anti-inflammatory [14], antiviral [15], anticarcinogenic [16], and immunomodulatory activities [15]. CAPE also inhibits enzymatic activities of endogenous and viral proteins [17–19] and transcriptional activity of NF-kappaB [14,20]. In addition, CAPE could suppress HCV replication enhanced by using the NF-kappaB activation activity of morphine [21], although it has been unknown which of moieties including CAPE is responsible for anti-HCV activity. Furthermore, it is not clear whether chemical modification of CAPE could enhance anti-HCV activity or not. In this report, we examined the effect of

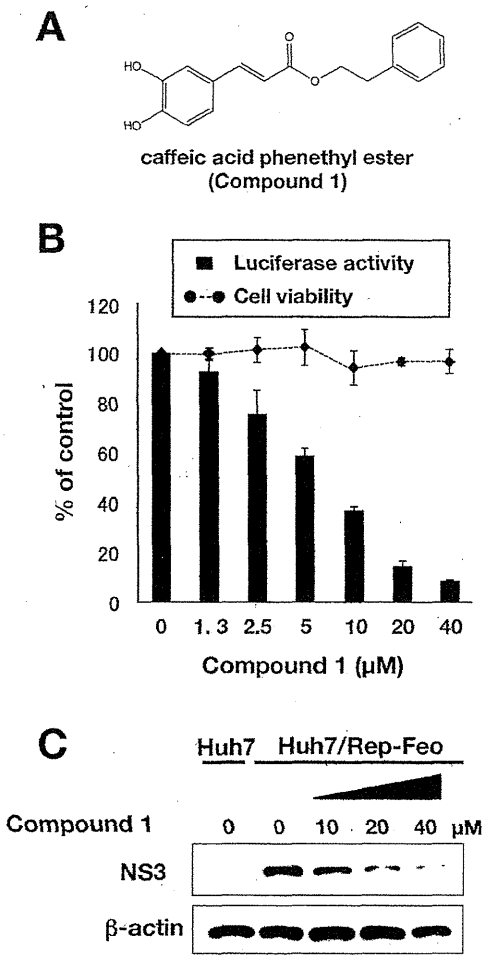

Figure 1. Effect of CAPE on viral replication in the replicon cell line of genotype 1b. (A) Molecular structure of CAPE. (B) Huh7/Rep-Feo cells were incubated for 72 h in a medium containing various concentrations of CAPE. Luciferase and cytotoxicity assays were carried out by the method described in Materials and Methods. Error bars indicate standard deviation. The data represent results from three independent experiments. (C) Protein extract was prepared from Huh7/Rep-Feo cells treated for 72 h with the indicated concentration of CAPE and it was then was subjected to Western blotting using antibodies to NS3 and beta-actin.
doi:10.1371/journal.pone.0082299.g001

CAPE derivatives on HCV proliferation to develop more effective and safer anti-HCV compounds.

Results

Effect of CAPE on HCV RNA replication in HCV subgenomic replicon cells

CAPE is composed of ester of caffeic acid and phenethyl alcohol (Fig. 1A). We examined the effect of CAPE (compound **1**) on both viral replication and cell growth in the HCV subgenomic replicon cell line Huh7/Rep-Feo. The replicon cell line was treated with various concentrations of compound **1**. The replication level of the HCV RNA was measured as an enzymatic activity of luciferase, which is bicistronically, encoded on the replicon RNA. Compound **1** suppressed HCV RNA replication at concentrations from 1.3 to 40 μM in a dose-dependent manner, but did not affect cell viability (Fig. 1B). HCV NS3, which is a viral protease, was decreased at the protein level by treatment with CAPE in a dose-dependent manner, corresponding to the viral replication, whereas beta-actin was not changed in the replicon cell line (Fig. 1C). Based on the calculation using a dose dependency of CAPE, compound **1** exhibited an EC_{50} value of 9.0 μM and a CC_{50} value of 136.1 μM, giving a selectivity index estimate (SI) of 17.9 (Table 1). These results suggest that treatment with CAPE inhibits HCV replication in HCV subgenomic replicon cells.

Structure-activity relationship of CAPE analogues

To clarify the structure-activity relationship of CAPE analogues, we examined the effect of hydroxyl groups on the aromatic ring (catechol moiety), the alkenyl moieties on alpha, beta-unsaturated esters, and the ester parts as follows (Figure S1).

We tested whether commercially available CAPE-related compounds **2** to **6** (Fig. S1) affected HCV replication (Table 1). All these compounds showed weaker inhibitory activity than CAPE (**1**), but are not toxic. Compound **2**, which is the acid component of CAPE, showed a slightly lower value of EC_{50} than compound **3**, which is the compound **2** derivative replaced a hydroxyl group with a methoxyl group of catechol moiety, while compound **4**, which is the derivative lacking two hydroxyl groups within catechol moiety, exhibits a higher value of EC_{50} than compounds **1** and **2**. These data suggest that the catechol moiety of CAPE is required for anti-HCV activity. Interestingly, compounds **5** and **6**, which are natural products including polyhydroxylated acid moieties in the ester parts, showed much weaker inhibitions than compound **1** and exhibits low *Clog P* values. The position of hydroxyl group or/and the structure of the ester part may affect the inhibitory activity and/or hydrophobicity.

We next examined the effects of caffeic acid ester compounds **7** to **11**, which include various lengths of alkyl side chains, on HCV replication (Table 2 and Figure S2). The EC_{50} values decreased in the order methyl ester (compound **7**), n-butyl ester (compound **8**), n-hexyl ester (compound **9**), and n-octyl ester (compound **10**), suggesting that elongation of the n-alkyl side chain increased the inhibitory activity. However, the EC_{50} value of n-dodecyl ester (compound **11**) was higher than that of compound **10**. Thus, n-octyl ester (compound **10**) showed the lowest EC_{50} value and the highest SI among the tested compounds shown in Tables 1 and 2. Compounds **7** to **11** gradually increased own *Clog P* values,

Table 1. Effect of CAPE (**1**) and related compounds **2–6** on HCV replication.

Compound (Number)	EC_{50} [a] (μM)	CC_{50} [b] (μM)	SI [c]	*Clog P* [d]
CAPE (**1**)	9.0±0.7	136.1±1.9	17.9	3.30
caffeic acid (**2**)	36.6±6.7	>320	>8.7	0.98
ferulic acid (**3**)	71.9±5.8	>320	>4.5	1.42
cinnamic acid henethyl ester (**4**)	86.1±6.3	>320	>3.7	4.56
chlorogenic acid (**5**)	103.0±3.4	>320	>3.1	−0.96
rosmarinic acid (**6**)	109.6±1.1	>320	>2.9	1.10

a: Fifty percent effective concentration based on the inhibition of HCV replication.
b: Fifty percent cytotoxicity concentration based on the reduction in cell viability.
c: Selectivity index (CC_{50}/EC_{50}).
d: Determined with ChemDraw software (Chem Bio Office Ultra, 2008).
doi:10.1371/journal.pone.0082299.t001

corresponding to length of n-alkyl side chain (Fig. 2A). Compounds **10** and **11** exhibit EC_{50} values of 2.7 and 5.9 μM, respectively, SI values of 29.6 and 9.80, respectively, and *Clog P* values of 4.90 and 5.96, respectively, suggesting that high hydrophobic property of n-alkyl side chain decreases anti-HCV activity. The appropriate *Clog P* value of caffeic acid ester containing unsaturated side chain may be around 5.

Dihydrocaffeic acid methyl ester (compound **12**) showed less activity than caffeic acid methyl ester (compound **7**) regardless of values of *Clog P* value and CC_{50}, suggesting that the alpha, beta-unsaturated part attached to ester affects the anti-HCV activity level (Table 3 and Figure S3).

We further examined the effect of the hydroxyl groups on the aromatic ring on HCV replication (Table 4 and Figure S4). The EC_{50} values of *O*-methylated caffeic acid n-octyl esters (compounds **13** and **14**) were higher than that of compound **10**. Compounds **15** including 3, 4-di-*O*-methylated caffeic acid n-octyl ester exhibited higher EC_{50} than values of compounds **10**, **13** and **14**. However, addition of a third hydroxyl group to 3, 4, 5-trihydroxy derivative (compound **16**) of compound **10** resulted in a reduction of anti-HCV activity. Furthermore, *Clog P* values of compound **10**, **13**, **14**, **15** and **16** were not correlated with anti-HCV activity (EC_{50} value) (Fig. 2B). These results suggest that the catechol moiety plays an important role in anti-HCV activity, and that the 4-hydroxy moiety is more important for the activity than the 3-hydroxy moiety.

Thus, compound **10**, which exhibits the lowest EC_{50} value and the highest SI value, is the most effective compound among CAPE analogues used in this study.

Effect of CAPE derivatives on virus production

The structure of compound **10** is shown in Fig. 3A. Treatment with compound **10** reduced HCV replication and NS3 protein in a dose-dependent manner at a higher anti-HCV level than

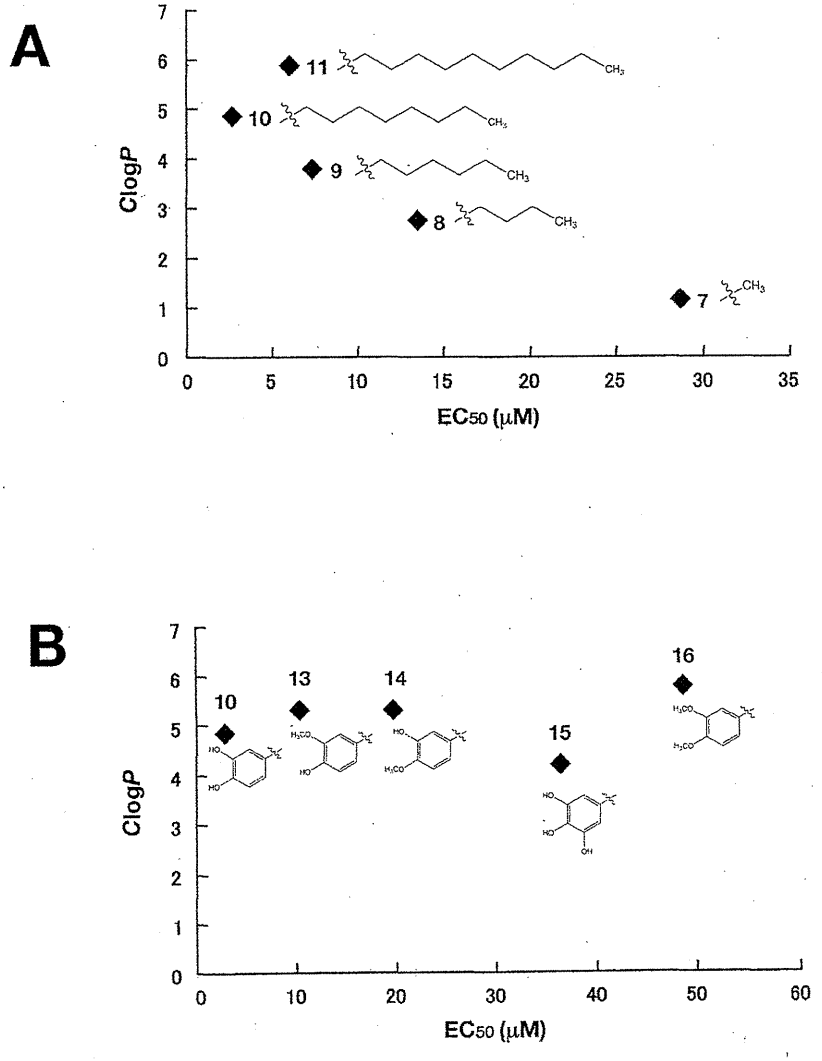

Figure 2. Correlation between the inhibitory effect on HCV replication *and* Clog *P* of CAPE analogues. Values of *x*-axis indicate EC_{50} values of CAPE analogues, while values of *y*-axis show Clog *P* values. (A) Correlation between the inhibitory effect on HCV replication and Clog *P* of CAPE analogues (Compound 7–11). (B) Correlation between the inhibitory effect on HCV replication and Clog *P* of CAPE analogues (Compound 10 and 13–16).

doi:10.1371/journal.pone.0082299.g002

Table 2. Effect of caffeic acid esters **7, 9–14**, including **1**, on HCV replication.

Compound No.	R	EC_{50} [a] (μM)	CC_{50} [b] (μM)	SI [c]	*Clog P* [d]
7	CH_3	28.6±1.2	122.1±5.0	4.2	1.20
8	C_4H_9	13.5±2.1	39.0±1.1	2.9	2.79
9	C_6H_{13}	7.3±0.2	37.6±1.2	5.1	3.85
10	C_8H_{17}	2.7±0.1	71.7±8.5	26.6	4.90
11	$C_{10}H_{21}$	5.9±0.9	57.9±2.9	9.8	5.96
1	$(CH_2)_2Ph$	9.0±0.7	136.1±1.9	17.9	3.30

The basic structure and side moieties are shown in Figure S2.
a: Fifty percent effective concentration based on the inhibition of HCV replication.
b: Fifty percent cytotoxicity concentration based on the reduction in cell viability.
c: Selectivity index (CC_{50}/EC_{50}).
d: Determined with ChemDraw software (Chem Bio Office Ultra, 2008).
doi:10.1371/journal.pone.0082299.t002

compound **1** (Figs. 3B and C), but not effect enzymatic activities of firefly and *Renilla* luciferases (Fig. 3D) and IRES-dependent translation (Fig. 3E), suggesting that inhibition of HCV replication by compound **10** is not due to offtarget effect. We evaluated the inhibitory effect of compound **10** on three different subgenomic replicon cell lines (1b: N strain, Con1 strain, 2a: JFH-1 strain) and one full genome replicon cell line (1b: O strain). Compound **10** inhibited the viral replication of all replicon cell lines at similar level, and exhibited the lowest EC_{50} value of 1.0 μM and an SI value of 63.1 by using Con1 replicon cells (Table 5). We next examined the effect of compound **10** on virus production by using HCVcc, since subgenomic replicon mimics HCV replication, but not the whole viral cycle. The Huh7 OK1 cell line, which is highly permissive to the HCV JFH1 strain [22], was infected with HCVcc and then treated with compound **10** at 24 h post-infection. The supernatant was harvested 72 h post-infection from the culture supernatant and then the RNA that prepared from the supernatant was estimated by real time qRT-PCR. Figure 3F shows that treatment with compound **10** reduced HCV viral production ($EC_{50}=1.8\pm0.4$ μM) in a similar way to the data obtained by using a replicon cell line. To clarify whether or not compound **10** inhibited HCV replication via interferon-signaling pathway, we analyzed ISRE activity and the expression of interferon stimulated gene (ISG) by using reporter assay and RT-PCR, respectively. The replicon cells were harvested at 48 h post-treatment. There were no significant effects of compound **1**, **6** and **10** on ISRE-promoter activities, while interferon alpha 2b significantly enhanced it as a positive control (Fig.4 A). The data of the RT-PCR analysis showed that the transcriptional expressions of ISGs including Mx1, MxA, IFIT4, ISG15, OAS1, OAS2, and OAS3 were induced with interferon alpha 2b, but not with compound **1**, **6** and **10** (Fig. 4B). These data suggest that the CAPE derivatives have an inhibitory effect on virus production and replication, irrespective of interferon signaling induction.

Synergistic effect of caffeic acid n-octyl ester on interferon and direct-acting antiviral agents

To estimate the effects of drug combinations on anti-HCV activity, we examined the antiviral activity of compound **10** in combination with IFN-α 2b, telaprevir (NS3 protease inhibitor), danoprevir (NS3 protease inhibitor), daclatasvir (NS5A inhibitor) or VX-222 (NS5B polymerase inhibitor). Con1 LUN· Sb #26 replicon cells were treated with compound **10** in combination with

Table 3. Effect of caffeic acid esters **7**and **8** on HCV replication.

Compound No.	EC_{50} [a] (μM)	CC_{50} [b] (μM)	SI [c]	*Clog P* [d]
7	28.6±1.2	122.1±5.0	4.2	1.20
12	77.0±1.6	140.7±3.4	1.8	1.02

Chemical structures of both compounds are shown in Figure S3
a: Fifty percent effective concentration based on the inhibition of HCV replication.
b: Fifty percent cytotoxicity concentration based on the reduction in cell viability.
c: Selectivity index (CC_{50}/EC_{50}).
d: Determined with ChemDraw software (Chem Bio Office Ultra, 2008).
doi:10.1371/journal.pone.0082299.t003

each anti-HCV agent at various concentration rations for 72 h. The effect of each drug combination on HCV replication was analyzed by using CalcuSyn. An explanatory diagram of isobologram was shown at a right end of lower panels of Fig. 5A as described in Materials and Methods. As shown in the resulting isobologram, all plots of the calculated EC_{90} values of compound **10** with IFN-alpha 2b, daclatasvir, or VX-222 are located under the additive line, while the plots of compound **10** with telaprevir, or danoprevir are located above the additive line and closed to the additive line (Fig. 5A). Additionally, we determined the degree of inhibition for each drug combination was analyzed as the combination index (CI) calculation at 50, 75 and 90% of effective concentrations by using CalcuSyn. An explanatory diagram was shown at a right end of lower panels of Fig. 5B as described in Materials and Methods. On the basis of the CalcuSyn analysis, the combination of compound **10** with daclatasvir exhibited strong synergistic effect on inhibition of HCV replication in the replicon cells (Fig. 5B, upper middle). The combination of compound **10** with VX-222 exhibited an additive to synergistic effect, suggesting that it trends toward synergistic (Fig. 5B, upper right), and with IFN-alpha 2b exhibited an antagonistic to synergistic effect, suggesting that it trends toward synergistic (Fig. 5B, upper left). In contrast, the combination of compound **10** with telaprevir resulted in antagonistic effect (Fig. 5B, lower left), and with danoprevir resulted in an antagonistic to additive effect, suggesting it trends toward antagonistic (Fig. 5B, lower middle). These calculated data

Table 4. Effect of octyl esters **10** and **13–16** on HCV replication.

Compound No.	R^1, R^2, R^3	EC_{50} [a] (μM)	CC_{50} [b] (μM)	SI [c]	*Clog P* [d]
10	$R^1=R^2=R^3=H$	2.7±0.1	71.7±8.5	26.6	4.90
13	$R^1=CH_3$, $R^2=R^3=H$	10.2±1.1	60.3±1.6	5.9	5.35
14	$R^1=R^3=H$, $R^2=CH_3$	19.6±0.8	59.2±1.4	3	5.35
15	$R^1=R^2=CH_3$, $R^3=H$	48.5±1.7	212.4±6.9	4.4	5.82
16	$R^1=R^2=H$, $R^3=OH$	36.3±2.9	59.8±6.9	1.6	4.24

The basic structure and side moieties are shown in Figure S4.
a: Fifty percent effective concentration based on the inhibition of HCV replication.
b: Fifty percent cytotoxicity concentration based on the reduction in cell viability.
c: Selectivity index (CC_{50}/EC_{50}).
d: Determined with ChemDraw software (Chem Bio Office Ultra, 2008).
doi:10.1371/journal.pone.0082299.t004

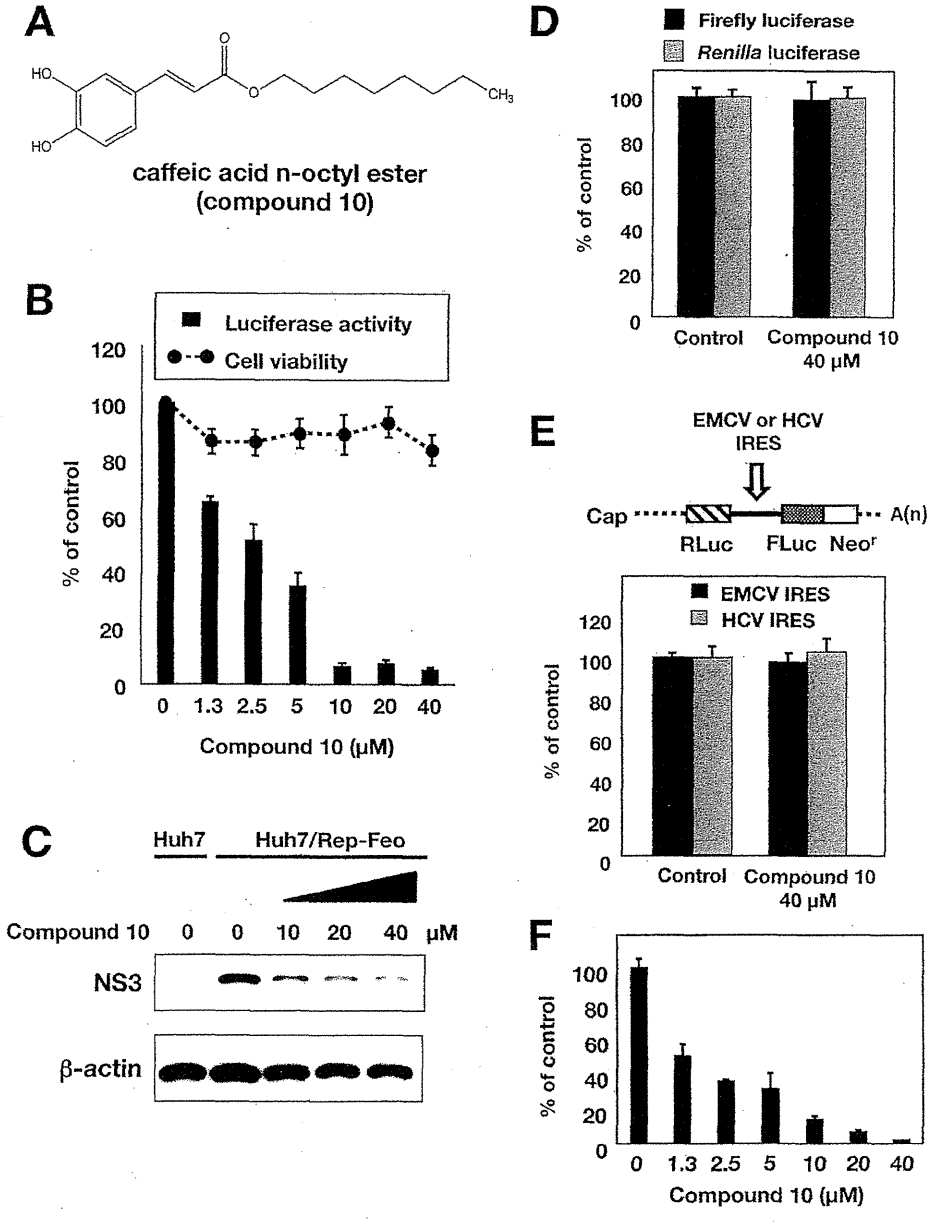

Figure 3. Effect of compound 10 on the viral replication in the replicon cell line and HCVcc. (A) Molecular structure of compound **10**. (B) Huh7/Rep-Feo cells were incubated for 72 h in a medium containing various concentrations of compound **10**. Luciferase and cytotoxicity assays were carried out by the method described in Materials and Methods. Error bars indicate standard deviation. The data represent three independent experiments. (C) Protein extract was prepared from Huh7/Rep-Feo cells treated for 72 h with the indicated concentration of compound **10** and it was then subjected to Western blotting using antibodies to NS3 and beta-actin. (D) Huh7 cell line was transfected with pEF Fluc IN encoding firefly luciferase or pEF Rluc IN encoding *Renilla* luciferase. Both transfected cell lines were incubated with DMSO (Control) or 40 μg/ml compound **10**. Firefly or *Renilla* luciferase activity was measured 72 h post-treatment. Luciferase activity was normalized with protein concentration. Error bars indicate standard deviation. The data were represented from three independent experiments. (E) Schematic structure of RNA transcribed from the plasmids was shown (Top). The bicistronic gene is transcribed under the control of elongation factor 1α (EF1α) promoter. The upstream cistron encoding *Renilla* luciferase (RLuc) is translated by a cap-dependent mechanism. The downstream cistron encodes the fusion protein (Feo), which consists of the firefly luciferase (Fluc) and neomycin phosphotransferase (Neo^r), and is translated under the control of the EMCV or HCV IRES. Huh7 cell line was transfected with each plasmid and incubated for 72 h post-treatment with DMSO (control) or 40 μg/ml of compound **10**. Firefly and *Renilla* luciferase activities were measured. Relative ratio of Firefly luciferase activity to *Renilla* luciferase activity was represented as percentage of the control condition. Error bars indicate standard deviation. The data were represented from three independent experiments. (F) Huh7 OK1 cell line was infected with HCVcc derived from JFH-1 strain and then treated with several concentrations of compound **10** at 24 h post-infection. The resulting cells were harvested 72 h post-infection. The viral RNA of supernatant was purified and estimated by the method described in Materials and Methods. Error bars indicate standard deviation. The data represent three independent experiments. Treatment with DMSO corresponds to '0'.
doi:10.1371/journal.pone.0082299.g003

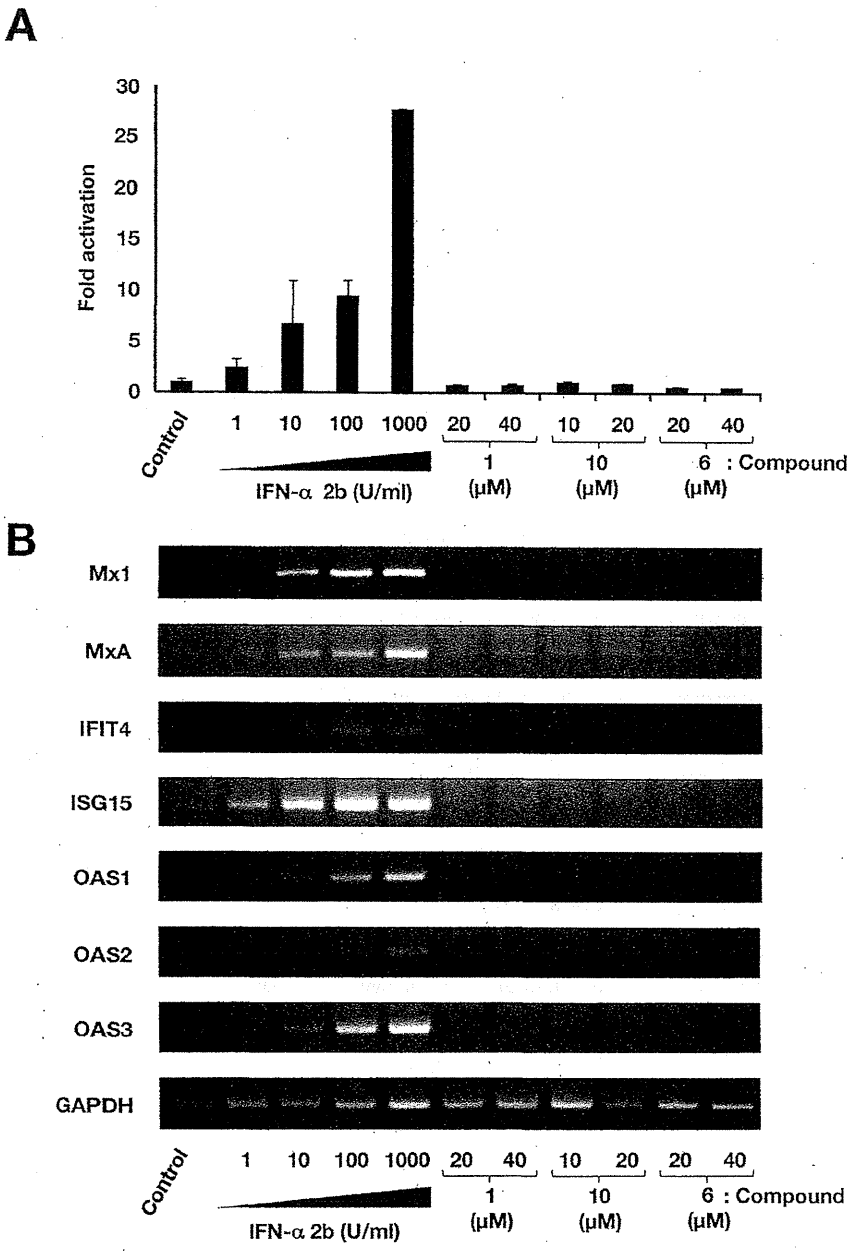

Figure 4. Effect of CAPE derivatives on the interferon-signaling pathway. (A) Plasmids pISRE-TA-Luc and phRG-TK were co-transfect into Huh7 OK1 cells. The transfected cells were cultured with 1, 10, 100, or 1000 U/mL of interferon-alpha 2b, and compounds **1**, **6** and **10**. Treatment with DMSO corresponds to '0'. After 48 h of treatment, luciferase activities were measured, and the value were normalized against *Renilla* luciferase activities. Error bars indicate standard deviation. The data represent three independent experiments. (B) Huh7 replicon cell line of genotype 1b was treated with 1, 10, 100, or 1000 U/mL of interferon-alpha 2b, and compounds **1**, **6** and **10** for 48 h. Treatment with DMSO corresponds to the control. The mRNAs of Mx1, MxA, IFIT4, ISG15, OAS1, OAS2, OAS3, and GAPDH as an internal control were detected by RT-PCR.
doi:10.1371/journal.pone.0082299.g004

of combination tests suggest that daclatasvir, IFN-alpha 2b, and VX-222 synergistically, but telaprevir and danoprevir antagonistically, inhibit HCV replication in combination with compound **10**.

Discussion

CAPE is an active component of propolis, which possesses broad-spectrum biological activities [14–19]. In this study, CAPE suppressed HCV RNA replication in a dose-dependent manner (Fig. 1A and B). Treatment with CAPE inhibited HCV replication with an EC_{50} of 9.0 μM and an SI of 17.9 in Huh7/Rep-Feo cells (Table 1). The treatment of the replicon cell line with CAPE did not induce expression of the IFN-inducible gene (Fig. 4), suggesting that the inhibition of HCV replication by CAPE is independent of the IFN signaling pathway.

Table 5. Anti-HCV activity of compound **10** in replicon cell lines of genotypes 1b and 2a.

Cell line	Replicon type	Strain (Genotype)	EC_{50} [a] (μM)	CC_{50} [b] (μM)	SI [c]
Huh7 Rep/Feo-1b	Subgenome	N (1b)	2.7±0.1	71.7±8.5	26.6
Con1 LUN Sb #26	Subgenome	Con1 (1b)	1.0±0.1	63.1±3.1	63.1
Huh7 Rep/Reo-2a	Subgenome	JFH1 (2a)	1.0±0.3	60.0±2.3	60.0
OR6	Full genome	O (1b)	1.5±0.4	61.7±0.6	41.1

a: Fifty percent effective concentration based on the inhibition of HCV replication.
b: Fifty percent cytotoxicity concentration based on the inhibition of HCV replication.
c: Selectivity Index (CC_{50}/EC_{50}).
doi:10.1371/journal.pone.0082299.t005

We also examined the effect of CAPE derivatives on HCV replication. Our data suggest that the n-alkyl side chain and catechol moiety of the CAPE derivative are critical in its anti-HCV activity (Tables 2 and 3). The EC_{50} value of the derivative decreased dependently on the length of the n-alkyl side chain until reaching octyl ester length (Table 2), while longer chains than octyl ester of a derivative led to an increase in the EC_{50} value and Clog *P* value. Compound **10**, Caffeic acid n-octyl ester, exhibited the highest anti-HCV activity among the tested compounds with an EC_{50} value of 2.7 μM and an SI value of 26.6. Cyclosporine A and its analogues could suppress the viral replication of genotype 1b at a higher level than that of genotype 2a [23]. Interestingly, compound **10** could inhibit HCV replication of genotype 1b and 2a at a similar level, irrespective of expression of the interferon-inducible gene (Fig. 4). CAPE and its derivatives may therefore possess a mechanism different from cyclosporine A and its analogues with respect to anti-HCV activity.

CAPE has been reported to be an inhibitor of NF-kappaB [14,20]. Lee et al. reported that the catechol moiety in CAPE was important for inhibition of NF-kappaB activation [24]. The data shown in Table 3 suggest that the catechol moiety in CAPE is critical to the anti-HCV activity of compound **10**. Previous studies have implicated the inhibition of NF-kappaB in anti-HCV activity. Treatment with an extract prepared from *Acacia confusa* [25] or San-Huang-Xie-Xin-Tang [26] could suppress HCV replication and inhibit NF-kappaB activation. However, Chen et al. reported that curcumin-mediated inhibition of NF-kappaB did not contribute to anti-HCV activity [11]. Furthermore, treatment with *N*'-(Morpholine-4carbonyloxy)-2(naphthalene-1-yl) acetimidamide could activate NF-kappaB and downstream gene expression in the same Huh7/Rep-Feo replicon cell line as the cell line used in this study and exhibited potent inhibition of HCV replication without interferon signaling [27]. These reports support the notion that CAPE derivatives do not mainly target NF-kappaB activity as part of their anti-HCV activity.

Several host proteins have been reported to regulate function of NS5A, leading to supporting HCV replication (review in [2,28]). Daclatasvir exhibited potent synergistic effect on anti-HCV activity in combination of compound **10** (Fig. 5). Anti-HCV activity of compound **10** might associate with intrinsic functions of host factors that interact with NS5A. NS3 protease inhibitors exhibited antagonistic effect in combination of compound **10** (Fig. 5). The inhibitory effect of compound **10** might be mediated by the activation of an unknown endogenous protease that is nonspecifically suppressed by NS3 protease inhibitors. Further study to clarify the mechanism by which compound **10** suppresses HCV replication might contribute to identification of a novel host factor as a drug target for development of the effective compound supporting an effect of other anti-HCV drugs.

In conclusion, we showed that CAPE and its analogue possess a significant inhibitory effect against HCV replication. The length of n-alkyl side chains and the catechol moiety of CAPE are critical to its inhibitory activity against HCV replication. The most effective derivative among the tested compounds was caffeic acid n-octyl ester, which exhibited an EC_{50} value of 1 μM and an SI value of 63.1 in the replicon cell line of genotype 1b strain Con1. Treatment with caffeic acid n-octyl ester reduced the viral replication of genotype 1b and 2a at a similar level and inhibited viral production of HCVcc. Treatment with caffeic acid n-octyl ester could synergistically enhance the anti-HCV activities of IFN-α 2b, daclatasvir, and VX-222, but neither telaprevir nor danoprevir. Further investigation to clarify the mechanism of anti-HCV activity and further modification of the compound to improve anti-HCV activity will lead to novel therapeutic strategies to treat chronic hepatitis C virus infection.

Materials and Methods

Compounds

Boldface numbers in this text indicate the compound numbers shown in Tables. All chemical structures of compounds used in this study are shown in figure S1. CAPE (**1**), caffeic acid (**2**), ferulic acid (**3**), and chlorogenic acid (**5**) and were purchased from Sigma-Aldrich (St. Louis, MO, USA). Cinnamic acid phenethyl ester (**4**) was from Tokyo Chemical Industry (Tokyo, Japan). Rosmarinic acid (**6**) was from Wako Pure Chemical (Tokyo, Japan). Caffeic acid n-octyl ester (n-octyl caffeate) (**10**), 3-O-methylcaffeic acid n-octyl ester (n-octyl-3-methylcaffeate) (**13**), 4-O-methylcaffeic acid n-octyl ester (n-octyl-3-methylcaffeate) (**14**), and 3, 4-O-dimethyl-caffeic acid n-octyl ester (n-octyl-3, 4-methylcaffeate) (**15**) were from LKT Laboratories (St. Paul, MN, USA).

Caffeic acid esters **7**, **8**, **9**, and **11** were synthesized by preparing caffeic acid chloride followed by treatment with corresponding alcohols [29]. Dihydrocaffeic acid ester **12** was prepared by hydrogenation of **7**. Compound **16** is a newly synthesized ester. Spectroscopic data of known esters **7–9**, and **11** prepared here were identical to those reported [30-32] Interferon alfa-2b (IFN-α 2b) was obtained from MSD (Tokyo, Japan). Telaprevir and daclatasvir were purchased from Selleckchem (Houston, TX, USA). Danoprevir and VX-222 were from AdooQ BioScience (Irvine, CA, USA).

Chemistry of 3,4,5-Trihydroxycinnamic acid n-octyl ester

3,4,5-Trihydroxycinnamic acid n-octyl ester (**16**) was prepared by condensation of corresponding benzaldehydes with malonic acid n-octyl monoester [33]. A solution of malonic acid n-octyl monoester (432 mg, 2 mmol), 3,4,5-trihydroxybenzaldehyde (462 mg, 3 mmol) and piperidine (0.2 mL) in pyridine (2 mL)

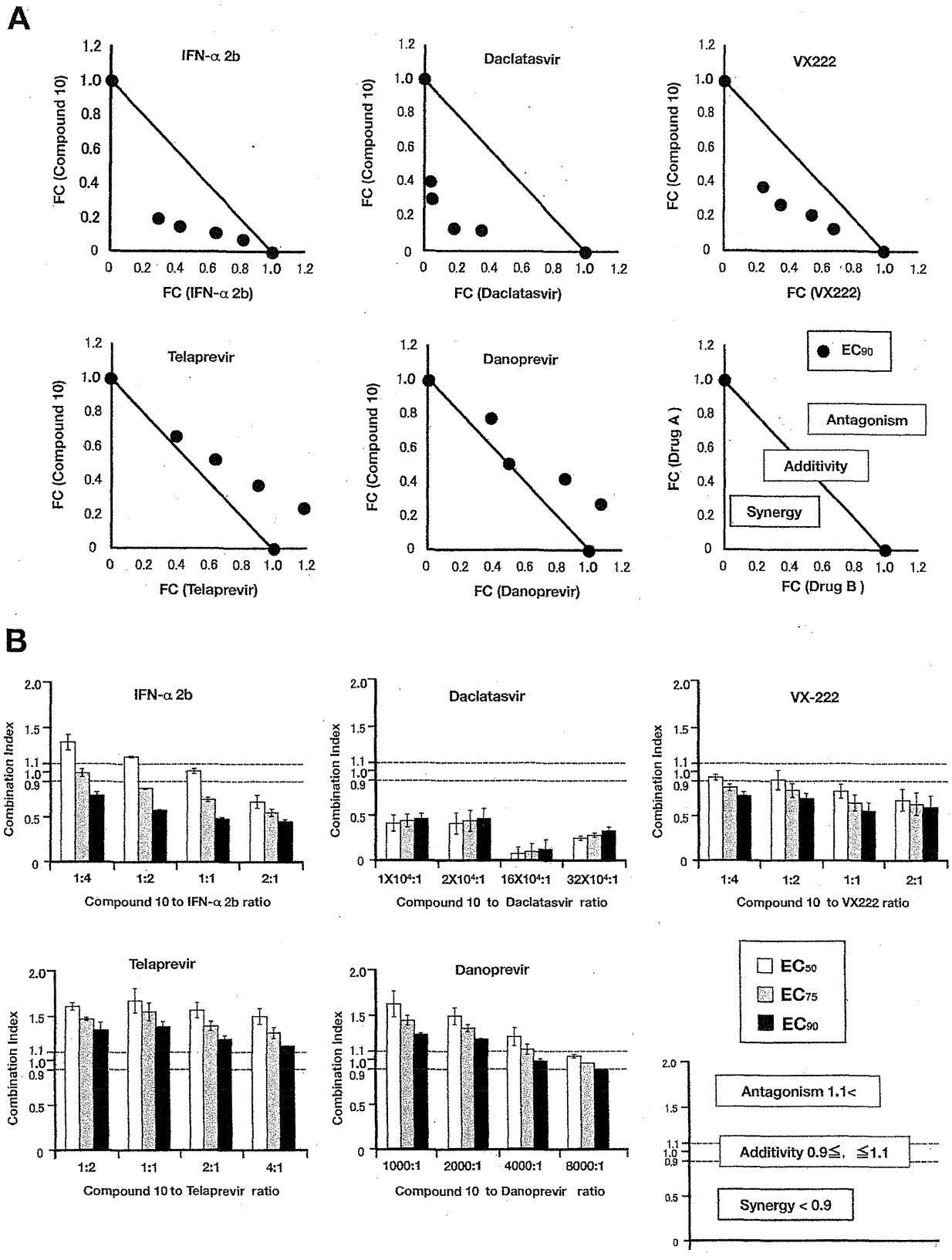
A
IFN-α 2b
FC (Compound 10)
FC (IFN-α 2b)
Daclatasvir
FC (Daclatasvir)
VX222
FC (VX222)
Telaprevir
FC (Telaprevir)
Danoprevir
FC (Danoprevir)
EC90
Antagonism
Additivity
Synergy
FC (Drug A)
FC (Drug B)
B
IFN-α 2b
Combination Index
1:4
1:2
1:1
2:1
Compound 10 to IFN-α 2b ratio
Daclatasvir
1X10⁴:1
2X10⁴:1
16X10⁴:1
32X10⁴:1
Compound 10 to Daclatasvir ratio
VX-222
Compound 10 to VX222 ratio
Telaprevir
1:2
1:1
2:1
4:1
Compound 10 to Telaprevir ratio
Danoprevir
1000:1
2000:1
4000:1
8000:1
Compound 10 to Danoprevir ratio
EC50
EC75
EC90
Antagonism 1.1<
Additivity 0.9≦, ≦1.1
Synergy < 0.9

Figure 5. Synergistic effect analyses for the combination of compound 10 with IFN-α 2b, daclatasvir, VX-222, telaprevir, or danoprevir. The Huh7 cell line, including the subgenomic replicon RNA of genotype 1b strain Con1, was treated for 72h with combinations of compound 10 and IFN-α 2b, daclatasvir, VX-222, telaprevir, or danoprevir. Luciferase assay were carried out as described in Materials and Methods. (A) The calculated EC_{90} values for combination were plotted as the fractional concentration (FC) of compound 10 and one of IFN-α 2b, daclatasvir, VX-222, telaprevir, and danoprevir on the *x* and *y* axes, respectively. Synergy, antagonism and additivity are indicated in a representative graph as a right end of lower graphs and are described in Materials and Methods. (B) Combination indexes of compound 10 with IFN-α 2b, daclatasvir, VX-222, telaprevir, or danoprevir at the EC50, EC75, and EC90 values were measured at various drug rations. Synergy, antagonism and additivity are indicated in a representative graph as a right end of lower graphs and are described in Materials and Methods.
doi:10.1371/journal.pone.0082299.g005

was heated at 70°C for 1 h. The reaction mixture was concentrated under a vacuum to give a residue, which was dissolved in $CHCl_3$-IPA (3:1, v/v) and then washed with 10% HCl and water. The organic layer was dried over Na_2SO_4 and evaporated to give a residue, which was purified by silica gel column chromatography using AcOEt-hexane (1:1, v/v) as eluent to give the corresponding n-octyl ester (85 mg, 13.8%) as a pale powder. FT-IR vmax (KBr): 3389, 3239, 2923, 1675, 1627, 1606 cm^{-1}. ^1H NMR (400MHz, CD_3OD) δ: 0.86 (3H, t, J= 7.2 Hz), 1.20–1.40 (10H, m), 1.65 (2H, quintet, J= 6.4 Hz), 4.11, (2H, t, J= 6.4 Hz), 6.16 (2H, d, J= 15.6 Hz), 6.55 (2H, s), 7.40 (2H, d, J= 15.6 Hz). 13C NMR (100 Hz, CD_3OD) δ: 14.4, 23.7, 27.1, 29.8, 30.3, 30.4, 32.9, 65.6, 108.5, 115.3, 126.6, 137.5, 147.1, 169.4. CI MS *m/z*: 309 (M^++H). High-resolution CI MS calcd. for $C_{17}H_{25}O_5$ (M^++H) for *309.1702*. Found: *309.1686*.

Replicon cell lines and virus infection

The Huh7/Rep-Feo cell line, which harbors the subgenomic replicon RNA composed of HCV IRES, the gene of the fusion protein consisting of neomycin phosphotransferase and firefly luciferase, EMCV IRES and a nonstructural gene of genotype 1b strain N in order in Huh7 cell line, was previously established [34]. Thus, the luciferase activity corresponds to the level of HCV RNA replication. The cell line was maintained in Dulbecco's modified Eagle medium containing 10% fetal calf serum and 0.5 mg/mL G418 and cultured in absence of G418 when they were treated with compounds. The Lunet/Con1LUN Sb #26 cell line, which harbors the subgenomic replicon RNA of the Con1 strain (genotype 1b), was described previously [35]. The OR6 cell line, which harbors the full genomic replicon RNA of the O strain (genotype 1b), was described previously [36]. The HCV replicon cell line derived from the genotype 2a strain JFH1 was described previously [37]. The viral RNA derived from the plasmid pJFH1 was transcribed and introduced into Huh7OK1 cells according to the method of Wakita et al. [38]. The virus was amplified by the several times passages. The cells were infected with the virus at a multiplicity of infection (moi) of 1 and then treated with each compound at 24 h post-infection. The culture supernatants were harvested 72 h post-treatment to estimate the viral RNA as described below.

Determination of luciferase activity in HCV replicon cells

The replicon cells were seeded at 2×10^4 cells per well in a 48-well plate 24 h before treatment. Compounds were added to the culture medium to give various concentrations. The resulting cells were harvested 72 h post-treatment and lysed with cell culture lysis reagent (Promega, Madison, WI). The luciferase activity of each cell lysate was estimated using a luciferase assay system (Promega). The resulting luminescence was detected by a Luminescencer-JNR AB-2100 (ATTO, Tokyo, Japan).

Determination of Cytotoxicity in HCV replicon cells

The replicon cells were seeded at a density of 1×10^4 cells per well in a 96-well plate and then incubated at 37°C for 24 h. Compounds were added to the culture medium to give various concentrations and were then harvested 72 h post-treatment. Cell viability was measured using a dimethylthiazol carboxymethoxyphenylsulfophenyl tetrazolium (MTS) assay with a CellTiter 96 aqueous one-solution cell proliferation assay kit (Promega).

Western Blotting

Western blotting was carried out by the method described previously [39]. The antibodies to NS3 (clone 8G-2, mousemonoclonal, Abcam, Cambridge, UK), and beta-actin were purchased from Cell Signaling Technology (rabbit polyclonal, Danvers, MA, USA) and were used as the primary antibodies in this study.

RNA analysis

Total RNAs were prepared from cells by using the RNAqueous-4PCR kit (Life Technologies, Carlsbad, CA). Viral RNA were prepared from culture supernatants by using the QIAamp Viral RNA mini kit (QIAGEN, Hilden, Germany). The viral RNA genome was estimated by the qRT-PCR method described previously [40]. RT-PCR was carried out by the method described previously [41] which was slightly modified at the PCR step. The PCR samples were incubated once for 10 min at 95°C for an initial activation step of the AmpliTaq Gold DNA Polymerase (Life Technologies), and then subjected to an amplification step of 30 repeats of the cycle consisting of three segments as follow: 0.5 min at 95°C, 1 min at 55°C and 1 min at 72°C. The primers used in this study were as follows: Mx1: 5′-AGCCACTGGACTGACGACTT-3′ and 5′-GAGGGCTGAAAATCCCTTTC-3′;

MxA: 5′-GTCAGGAGTTGCCCTTCCCA-3′ and 5′-ATTCCCATTCCTTCCCCGG-3′;

IFIT4: 5′-CCCTTCAGGCATAGGCAGTA-3′ and 5′-CTCCTACCCGTCACAACCAC -3′; ISG15: 5′-CGCAGATCACCCAGAAGAT-3′ and 5′-GCCCTTGTTATTCCTCACCA-3′;

OAS1: 5′-CAAGCTCAAGAGCCTCATCC-3′ and 5′-TGGGCTGTGTTGAAATGTGT-3′;

OAS2: 5′-ACAGCTGAAAGCCTTTTGGA-3′ and 5′-GCATTAAAGGCAGGAAGCAC-3′;

OAS3: 5′-CACTGACATCCCAGACGATG-3′ and 5′-GATCAGGCTCTTCAGCTTGGC-3′;

GAPDH: 5′-GAAGGTGAAGGTCGGAGTC and 5′- GAAGATGGTGATGGGATTTC-3′

Effects on activities of internal ribosome entry site (IRES) and luciferases

Huh7 OK1 cells were transfected with pEF.Rluc.HCV.IRES.-Feo or pEF.Rluc.EMCV.IRES.Feo [39]. These transfected cells were seeded at 2×10^4 cells per well in a 48-well plate 24 h before treatment, treated with DMSO or compound **10**, and then harvested at 72 h post-treatment. The firefly luciferase activities were measured with a luciferase assay system (Promega). The total protein concentration was measured using the BCA Protein Assay Reagent Kit (Thermo Scientific, Rockford, IL, USA) to normalize

luciferase activity. To evaluate the interferon response, Huh7OK1 cells were seeded on a 48 well plate at a density of 2×10^4 cells per well, and transfected with pISRE-TA-Luc (Takara bio, Shiga, Japan) and phRG-TK (Promega). These transfected cells were incubated in the presence of compounds, IFN-α 2b, or DMSO, and then harvested at 48 h post-treatment. The firefly luciferase and *Renilla* luciferase activities were quantified by using Dual luciferase reporter assay system (Promega).

Prediction of Clog*P* for compounds

The *ClogP* value deduced from chemical structure roughly corresponds to a value of hydrophobicity. The *ClogP* values of compounds used in this study were calculated using the computer software Chem Bio Office Ultra 2008 (PerkinElmer, Cambridge, MA, USA).

Synergistic effect of caffeic acid n-octyl ester on anti-HCV activities of other drugs

The effects of drug-drug combinations were evaluated by using the Con1 LUN Sb #26 replicon cells, and were analyzed by using the computer software CalcuSyn (Biosoft, Cambridge, United Kingdom). Dose inhibition curves of two different drugs were plotted with each other. In each drug combination, EC_{90} values of several combinations of two different drugs were plotted as the fractional concentration (FC) of both drugs on the *x* and *y*-axes. Additivity indicates the line linked between 1.0 FC value points of both drugs in the absence of each other. Synergy and antagonism are indicated by values plotted under and above, respectively, an additivity line. The explanatory diagram of isobologram is shown in a right end of lower panels of Figure 5A. Combination indexes (CIs) were calculated at the EC_{50}, EC_{75}, and EC_{90} by using CalcuSyn. A CI value of less than 0.9 indicates synergy. A CI value ranging from 0.9 to 1.1 indicates additivity. A CI value of more than 1.1 indicates antagonism. The explanatory diagram was shown in a right end of lower panels of Figure 5B.

Supporting Information

Figure S1 Molecular structure of CAPE and commercial CAPE-related compounds. CAPE structure is divided into three parts: (I) the catechol moiety, (II) the alkenyl moiety on alpha, beta -unsaturated ester, and (III) the ester part. Molecular structures of CAPE and its commercial derivatives are shown.
(TIF)

Figure S2 The basic structure and side moieties of compounds shown in Table 2. Each compound structure is represented on the basis of the basic structure (top).
(TIF)

Figure S3 The molecular structures of compounds 7 and 12, which are shown in Table 3. Both compounds are different in alpha, beta-unsaturated or saturated part attached to ester.
(TIF)

Figure S4 The basic structure and side moieties of compounds shown in Table 4. Each compound structure is represented on the basis of the basic structure (top).
(TIF)

Acknowledgments

We thank T. Wakita for kindly providing a plasmid.

Author Contributions

Conceived and designed the experiments: MT KM. Performed the experiments: H. Shen AY MN HY MS H. Shindo SM. Analyzed the data: HK TT NE. Contributed reagents/materials/analysis tools: YF MI NK NS. Wrote the paper: H. Shen AY MT KM.

References

1. Baldo V, Baldovin T, Trivello R, Floreani A (2008) Epidemiology of HCV infection. Curr Pharm Des 14: 1646–1654.
2. Moriishi K, Matsuura Y (2012) Exploitation of lipid components by viral and host proteins for hepatitis C virus infection. Front Microbiol 3: 54.
3. Hijikata M, Kato N, Ootsuyama Y, Nakagawa M, Shimotohno K (1991) Gene mapping of the putative structural region of the hepatitis C virus genome by in vitro processing analysis. Proc Natl Acad Sci USA 88: 5547–5551.
4. Lohmann V, Korner F, Koch J, Herian U, Theilmann L, et al. (1999) Replication of subgenomic hepatitis C virus RNAs in a hepatoma cell line. Science 285: 110–113.
5. Hofmann WP, Zeuzem S (2011) A new standard of care for the treatment of chronic HCV infection. Nat Rev Gastroenterol Hepatol 8: 257–264.
6. Jacobson IM, McHutchison JG, Dusheiko G, Di Bisceglie AM, Reddy KR, et al. (2011) Telaprevir for previously untreated chronic hepatitis C virus infection. N Engl J Med 364: 2405–2416.
7. Sarrazin C, Hezode C, Zeuzem S, Pawlotsky JM (2012) Antiviral strategies in hepatitis C virus infection. J Hepatol 56 Suppl 1: S88–100.
8. Kieffer TL, Kwong AD, Picchio GR (2010) Viral resistance to specifically targeted antiviral therapies for hepatitis C (STAT-Cs). J Antimicrob Chemother 65: 202–212.
9. Ahmed-Belkacem A, Ahnou N, Barbotte L, Wychowski C, Pallier C, et al. (2010) Silibinin and related compounds are direct inhibitors of hepatitis C virus RNA-dependent RNA polymerase. Gastroenterology 138: 1112–1122.
10. Calland N, Albecka A, Belouzard S, Wychowski C, Duverlie G, et al. (2012) (-)-Epigallocatechin-3-gallate is a new inhibitor of hepatitis C virus entry. Hepatology 55: 720–729.
11. Chen MH, Lee MY, Chuang JJ, Li YZ, Ning ST, et al. (2012) Curcumin inhibits HCV replication by induction of heme oxygenase-1 and suppression of AKT. Int J Mol Med 30: 1021–1028.
12. Bachmetov L, Gal-Tanamy M, Shapira A, Vorobeychik M, Giterman-Galam T, et al. (2012) Suppression of hepatitis C virus by the flavonoid quercetin is mediated by inhibition of NS3 protease activity. J Viral Hepat 19: e81–88.
13. Takeshita M, Ishida Y, Akamatsu E, Ohmori Y, Sudoh M, et al. (2009) Proanthocyanidin from blueberry leaves suppresses expression of subgenomic hepatitis C virus RNA. J Biol Chem 284: 21165–21176.
14. Toyoda T, Tsukamoto T, Takasu S, Shi L, Hirano N, et al. (2009) Anti-inflammatory effects of caffeic acid phenethyl ester (CAPE), a nuclear factor-kappaB inhibitor, on Helicobacter pylori-induced gastritis in Mongolian gerbils. Int J Cancer 125: 1786–1795.
15. Ho CC, Lin SS, Chou MY, Chen FL, Hu CC, et al. (2005) Effects of CAPE-like compounds on HIV replication in vitro and modulation of cytokines in vivo. J Antimicrob Chemother 56: 372–379.
16. Chiao C, Carothers AM, Grunberger D, Solomon G, Preston GA, et al. (1995) Apoptosis and altered redox state induced by caffeic acid phenethyl ester (CAPE) in transformed rat fibroblast cells. Cancer Res 55: 3576–3583.
17. Boudreau LH, Maillet J, LeBlanc LM, Jean-Francois J, Touaibia M, et al. (2012) Caffeic acid phenethyl ester and its amide analogue are potent inhibitors of leukotriene biosynthesis in human polymorphonuclear leukocytes. PLoS One 7: e31833.
18. Lee KW, Chun KS, Lee JS, Kang KS, Surh YJ, et al. (2004) Inhibition of cyclooxygenase-2 expression and restoration of gap junction intercellular communication in H-ras-transformed rat liver epithelial cells by caffeic acid phenethyl ester. Ann N Y Acad Sci 1030: 501–507.
19. Fesen MR, Kohn KW, Leteurtre F, Pommier Y (1993) Inhibitors of human immunodeficiency virus integrase. Proc Natl Acad Sci U S A 90: 2399–2403.
20. Natarajan K, Singh S, Burke TR Jr, Grunberger D, Aggarwal BB (1996) Caffeic acid phenethyl ester is a potent and specific inhibitor of activation of nuclear transcription factor NF-kappa B. Proc Natl Acad Sci U S A 93: 9090–9095.
21. Li Y, Zhang T, Douglas SD, Lai JP, Xiao WD, et al. (2003) Morphine enhances hepatitis C virus (HCV) replicon expression. Am J Pathol 163: 1167–1175.
22. Okamoto T, Omori H, Kaname Y, Abe T, Nishimura Y, et al. (2008) A single-amino-acid mutation in hepatitis C virus NS5A disrupting FKBP8 interaction impairs viral replication. J Virol 82: 3480–3489.
23. Ishii N, Watashi K, Hishiki T, Goto K, Inoue D, et al. (2006) Diverse effects of cyclosporine on hepatitis C virus strain replication. J Virol 80: 4510–4520.

24. Lee Y, Shin DH, Kim JH, Hong S, Choi D, et al. (2010) Caffeic acid phenethyl ester-mediated Nrf2 activation and IkappaB kinase inhibition are involved in NFkappaB inhibitory effect: structural analysis for NFkappaB inhibition. Eur J Pharmacol 643: 21–28.
25. Lee JC, Chen WC, Wu SF, Tseng CK, Chiou CY, et al. (2011) Anti-hepatitis C virus activity of Acacia confusa extract via suppressing cyclooxygenase-2. Antiviral Res 89: 35–42.
26. Lee JC, Tseng CK, Wu SF, Chang FR, Chiu CC, et al. (2011) San-Huang-Xie-Xin-Tang extract suppresses hepatitis C virus replication and virus-induced cyclooxygenase-2 expression. J Viral Hepat 18: e315–324.
27. Kusano-Kitazume A, Sakamoto N, Okuno Y, Sekine-Osajima Y, Nakagawa M, et al. (2012) Identification of novel N-(morpholine-4-carbonyloxy) amidine compounds as potent inhibitors against hepatitis C virus replication. Antimicrob Agents Chemother 56: 1315–1323.
28. Moradpour D, Penin F, Rice CM (2007) Replication of hepatitis C virus. Nat Rev Microbiol 5: 453–463.
29. Lee YJ, Liao PH, Chen WK, Yang CY (2000) Preferential cytotoxicity of caffeic acid phenethyl ester analogues on oral cancer cells. Cancer Lett 153: 51–56.
30. Bourne GT, Golding SW, McGeary RP, Meutermans WD, Jones A, et al. (2001) The development and application of a novel safety-catch linker for BOC-based assembly of libraries of cyclic peptides. J Org Chem 66: 7706–7713.
31. Nagaoka T, Banskota AH, Tezuka Y, Saiki I, Kadota S (2002) Selective antiproliferative activity of caffeic acid phenethyl ester analogues on highly liver-metastatic murine colon 26-L5 carcinoma cell line. Bioorg Med Chem 10: 3351–3359.
32. Uwai K, Osanai Y, Imaizumi T, Kanno S, Takeshita M, et al. (2008) Inhibitory effect of the alkyl side chain of caffeic acid analogues on lipopolysaccharide-induced nitric oxide production in RAW264.7 macrophages. Bioorg Med Chem 16: 7795–7803.
33. Zhang Z, Xiao B, Chen Q, Lian XY (2010) Synthesis and biological evaluation of caffeic acid 3,4-dihydroxyphenethyl ester. J Nat Prod 73: 252–254.
34. Yokota T, Sakamoto N, Enomoto N, Tanabe Y, Miyagishi M, et al. (2003) Inhibition of intracellular hepatitis C virus replication by synthetic and vector-derived small interfering RNAs. EMBO Rep 4: 602–608.
35. Frese M, Barth K, Kaul A, Lohmann V, Schwarzle V, et al. (2003) Hepatitis C virus RNA replication is resistant to tumour necrosis factor-alpha. Journal of General Virology 84: 1253–1259.
36. Ikeda M, Abe K, Dansako H, Nakamura T, Naka K, et al. (2005) Efficient replication of a full-length hepatitis C virus genome, strain O, in cell culture, and development of a luciferase reporter system. Biochem Biophys Res Commun 329: 1350–1359.
37. Nishimura-Sakurai Y, Sakamoto N, Mogushi K, Nagaie S, Nakagawa M, et al. (2010) Comparison of HCV-associated gene expression and cell signaling pathways in cells with or without HCV replicon and in replicon-cured cells. J Gastroenterol 45: 523–536.
38. Wakita T, Pietschmann T, Kato T, Date T, Miyamoto M, et al. (2005) Production of infectious hepatitis C virus in tissue culture from a cloned viral genome. Nat Med 11: 791–796.
39. Yamashita A, Salam KA, Furuta A, Matsuda Y, Fujita O, et al. (2012) Inhibition of hepatitis C virus replication and NS3 helicase by the extract of the feather star *Alloeocomatella polycladia*. Mar Drugs 10: 744–761.
40. Fujimoto Y, Salam KA, Furuta A, Matsuda Y, Fujita O, et al. (2012) Inhibition of Both Protease and Helicase Activities of Hepatitis C Virus NS3 by an Ethyl Acetate Extract of Marine Sponge Amphimedon sp. PLoS One 7: e48685.
41. Jin H, Yamashita A, Maekawa S, Yang PT, He LM, et al. (2008) Griseofulvin, an oral antifungal agent, suppresses hepatitis C virus replication in vitro. Hepatology Research 38: 909–918.

Journal of proteome research

Article

pubs.acs.org/jpr

Understanding the Biological Context of NS5A–Host Interactions in HCV Infection: A Network-Based Approach

Lokesh P. Tripathi,*[,¶,†] Hiroto Kambara,[¶,‡] Yi-An Chen,[†] Yorihiro Nishimura,[‡] Kohji Moriishi,[‡] Toru Okamoto,[‡] Eiji Morita,[‡] Takayuki Abe,[‡] Yoshio Mori,[‡] Yoshiharu Matsuura,[‡] and Kenji Mizuguchi*[,†,§]

[†]National Institute of Biomedical Innovation, 7-6-8 Saito Asagi, Ibaraki, Osaka, 567-0085, Japan

[‡]Department of Molecular Virology, Research Institute for Microbial Diseases, Osaka University, 3-1 Yamada-Oka, Suita, Osaka, 565-0871, Japan

[§]Graduate School of Frontier Biosciences, Osaka University, 1-3 Yamada-Oka, Suita, Osaka, 565-0871, Japan

Supporting Information

ABSTRACT: Hepatitis C virus (HCV) is a major cause of chronic liver disease. HCV NS5A protein plays an important role in HCV infection through its interactions with other HCV proteins and host factors. In an attempt to further our understanding of the biological context of protein interactions between NS5A and host factors in HCV pathogenesis, we generated an extensive physical interaction map between NS5A and cellular factors. By combining a yeast two-hybrid assay with comprehensive literature mining, we built the NS5A interactome composed of 132 human proteins that interact with NS5A. These interactions were integrated into a high-confidence human protein interactome (HPI) with the help of the TargetMine data warehouse system to infer an overall protein interaction map linking NS5A with the components of the host cellular networks. The NS5A–host interactions that were integrated with the HPI were shown to participate in compact and well-connected cellular networks. Functional analysis of the NS5A "infection" network using TargetMine highlighted cellular pathways associated with immune system, cellular signaling, cell adhesion, cellular growth and death among others, which were significantly targeted by NS5A–host interactions. In addition, cellular assays with in vitro HCV cell culture systems identified two ER-localized host proteins RTN1 and RTN3 as novel regulators of HCV propagation. Our analysis builds upon the present understanding of the role of NS5A protein in HCV pathogenesis and provides potential targets for more effective anti-HCV therapeutic intervention.

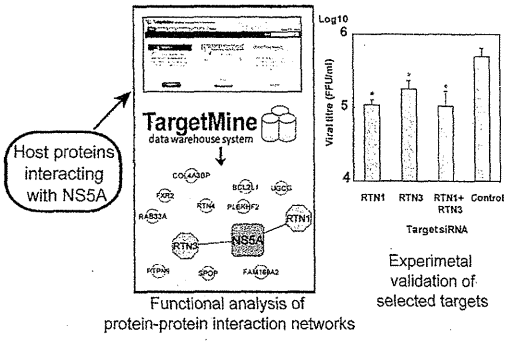

KEYWORDS: *HCV, NS5A, host–pathogen protein–protein interactions, biological network analysis, literature mining, pathway enrichment analysis, siRNA knockdown, target discovery, TargetMine, yeast two-hybrid*

INTRODUCTION

Hepatitis C virus (HCV) causes chronic liver disease including liver steatosis, cirrhosis and hepatocellular carcinoma (HCC) and infects nearly 3% of the world population. HCV possesses a single-stranded RNA genome encoding a 3000 amino acid polyprotein, which is processed by host and viral proteases to yield 10 viral proteins, Core, E1, E2, p7, NS2, NS3, NS4A, NS4B, NS5A and NS5B.[1−5] HCV variants are classified into seven genotypes that display phylogenetic heterogeneity, differences in infectivity and interferon sensitivity.[6,7] However, despite considerable research, a precise understanding of the molecular mechanisms underlying HCV pathology remains elusive.

HCV NS5A protein (hereafter referred to as NS5A) is a RNA binding phosphoprotein, which consists of three domains; domain I includes a zinc-finger motif necessary for HCV replication and an N-terminal membrane anchor region, and the unstructured domains II and III facilitate protein–protein interactions. NS5A plays a critical role in regulating viral replication, production of infectious viral particles, interferon resistance and modulation of apoptosis in HCV pathogenesis via interactions with other HCV proteins and host factors.[8−12] Furthermore, BMS-790052, a small molecule inhibitor of NS5A, is the most potent inhibitor of HCV infection known so far.[13] Consequently, NS5A has emerged as a unique, attractive and promising target for anti-HCV therapy.[14−19] In particular, impairing interactions between NS5A and host factors has been shown to impede HCV infection, which may offer novel anti-HCV therapeutic approaches.[12,20] However, the overall structure and precise functions of NS5A in HCV pathogenesis are poorly understood.

Pathogens such as viruses infect their hosts by interacting with the components of the host cellular networks and

Received: November 30, 2012
Published: May 6, 2013

   dx.doi.org/10.1021/pr3011217 | J. Proteome Res. 2013, 12, 2537−2551

exploiting the cellular machinery for their survival and propagation. Therefore, elucidating host–pathogen interactions is crucial for a better understanding of pathogenesis.[21−26] Here, we report the host biological processes likely to be influenced by NS5A by virtue of an inferred protein–protein interaction (PPI) network. We describe our integrated approach that combines an experimental yeast two-hybrid (Y2H) assay using NS5A as bait to screen a library of human cDNAs with comprehensive literature mining. The analysis of the NS5A infection network illustrates the functional pathways likely to be influenced by NS5A–host interactions in HCV pathogenesis, thus providing novel insights into the NS5A function in HCV pathogenesis. Furthermore, RTN1 and RTN3, which are endoplasmic reticulum (ER)-localized proteins involved in regulating ER integrity, will be demonstrated as novel regulators of HCV propagation and thus attractive targets for anti-HCV therapy.

MATERIALS AND METHODS

Yeast Two-Hybrid Protein Assay

Screening for the genes encoding host proteins that interact with NS5A was performed using the Matchmaker two-hybrid system (Clontech, Palo Alto, CA, USA) as per the manufacturers' specifications. Human adult liver libraries were purchased from Clontech and were cloned into the pAct2 vector (Clontech) and expressed as fusion proteins fused to the Gal4-activation domain (Gal4-AD). Since Y2H requires the bait protein to translocate to the nucleus, the cDNA of the region corresponding to the NS5A encoding amino acids 1973–2419 (excluding the NS5A N-terminal membrane anchor region) within the HCV polyprotein from the J1 strain (genotype 1b)[27] was amplified by polymerase chain reaction (PCR) and was cloned into the pGBKT7 vector (Clontech)[28] and expressed as Gal4-DNA binding domain (Gal4-DB) fusion in the AH109 yeast strain. The human liver libraries were subsequently screened by Y2H using NS5A as bait. A total of 4×10^6 transformants were screened in this manner, and the positive clones (see Supporting Information) were isolated and sequenced to identify the genes coding for the NS5A interacting host factors (Supporting Information, Table S1).

Literature Mining for Pairwise NS5A–Human Interactions

Literature information describing pairwise interactions between NS5A and cellular proteins were extracted from Medline using the PubMed interface and two other information retrieval and extraction tools, EBIMed[29] and Protein Corral. These tools employ an automatic text-mining approach, but we supplemented them with a follow-up manual inspection. All abstracts related to "NS5A" and "HCV NS5A" keywords and interaction verbs (including "interact", "bind", "attach", "associate")[30] were gathered and manually examined to retrieve direct pairwise NS5A–human protein interactions (see Supporting Information, Tables S2, S3, S4, S5a).

Construction of Extended Protein–Protein Interaction Networks

Physical and direct binary interactions between all human proteins were retrieved from BioGRID 3.1.93[31] and iRefindex 9.0[32] databases using TargetMine.[33] TargetMine is an integrated data warehouse that combines different types of biological data and employs an objective protocol to prioritise candidate genes for further experimental investigation.[33] The interactions were filtered for redundancy, potential false positives and isolated components to infer a representative undirected and singly connected high-confidence human protein interactome (HPI) comprising 22 532 nonredundant binary physical interactions between 7277 proteins (see Supporting Information, Figure S2, Table S5b). The inferred HPI was used to identify biologically relevant trends, the significance of which was assessed by using randomized networks (see below). Secondary interactors of the NS5A interacting proteins were retrieved from the HPI and were appended to the NS5A–host interactions to construct a representative NS5A infection network (Supporting Information, Table S5a).

Topological Analysis

Network components were visualized using Cytoscape,[34,35] while network properties such as *node degree distribution, average shortest path* and *betweenness* measures were computed using Cytoscape NetworkAnalyzer plugin[36] as described earlier.[24] For comparison, degree preserved randomized PPI networks were generated by edge rewiring using the Cytoscape RandomNetworks plugin and were used as control networks to assess the statistical significance of the topological trends observed in the inferred PPI networks (see Supporting Information).

Functional Analysis by Characterization of Enriched Biological Associations

Protein structural domain assignments were retrieved from the Gene3D database,[37] Gene ontology associations from the GO consortium,[38] and biological pathway data from KEGG[39] were used to assign functional annotations to the genes in the NS5A infection network. The enrichment of specific biological associations within the NS5A infection network was estimated by performing the hypergeometric test within TargetMine. The inferred p-values were further adjusted for multiple test correction to control the false discovery rate using the Benjamini and Hochberg procedure,[40,41] and the annotations/pathways were considered significant if the adjusted $p \leq 0.005$.

RNAi and Transfection

A mixture of four siRNA targets each to RTN1 and RTN3 (SMARTpool:siGENOME RTN1 siRNA and SMARTpool:siGENOME RTN3 siRNA, respectively) were purchased from Thermo Scientific (Thermo Scientific, Waltham, MA, USA). siGENOME Non-Targeting siRNA Pool #1 (Thermo Scientific) was used as a control siRNA. Thermo Scientific ID numbers of siRNA mixtures of RTN1 and RTN3 and the control were M-014138-00, M-020088-00 and D-001206-13-05, respectively. Each siRNA mixture was introduced into the cell lines by using lipofectamine RNAiMax (Invitrogen, Carlsbad, CA, USA). The replicon cell line, as will be described below, was transfected with each siRNA at a final concentration of 20 nM as per the manufacturer's protocol and then seeded at 2.5×10^4 cells per well of a 24-well plate. The transfected cells were harvested at 72 h post-transfection. The Huh7OK1 cell line, as will be described below, was transfected with each siRNA at a final concentration of 20 nM as per the manufacturer's protocol and then seeded at 2.5×10^4 cells per well of a 24-well plate. The transfected cells were infected with JFH1 at an MOI of 0.05 at 24 h post-transfection. The resulting cells were harvested at the indicated time.

Table 1. List of 132 Human Proteins Interacting with the HCV NS5A Protein

gene ID	symbol	description	refs
47	ACLY	ATP citrate lyase	22
60	ACTB	actin, beta	101
79026	AHNAK	AHNAK nucleoprotein	22
10598	AHSA1	AHA1, activator of heat shock 90 kDa protein ATPase homologue 1 (yeast)	102
207	AKT1	v-akt murine thymoma viral oncogene homologue 1	22
302	ANXA2	annexin A2	103
335	APOA1	apolipoprotein A-I	22
348	APOE	apolipoprotein E	22
116985	ARAP1	ArfGAP with RhoGAP domain, ankyrin repeat and PH domain 1	22
27236	ARFIP1	ADP-ribosylation factor interacting protein 1	22
23204	ARL6IP1	ADP-ribosylation factor-like 6 interacting protein 1	this study
4508	ATP6	ATP synthase F0 subunit 6	this study
8312	AXIN1	axin 1	22
581	BAX	BCL2-associated X protein	22
222389	BEND7	BEN domain containing 7	22
274	BIN1	bridging integrator 1	this study; [22,47]
89927	C16orf45	chromosome 16 open reading frame 45	this study
8618	CADPS	Ca^{++}-dependent secretion activator	22
93664	CADPS2	Ca^{++}-dependent secretion activator 2	22
79080	CCDC86	coiled-coil domain containing 86	22
983	CDK1	cyclin-dependent kinase 1	22
1021	CDK6	cyclin-dependent kinase 6	22
1060	CENPC1	centromere protein C 1	22
153241	CEP120	centrosomal protein 120 kDa	22
11190	CEP250	centrosomal protein 250 kDa	22
9702	CEP57	centrosomal protein 57 kDa	22
80254	CEP63	centrosomal protein 63 kDa	22
1381	CRABP1	cellular retinoic acid binding protein 1	22
1445	CSK	c-src tyrosine kinase	22
1452	CSNK1A1	casein kinase 1, alpha 1	104
1457	CSNK2A1	casein kinase 2, alpha 1 polypeptide	63,105
1499	CTNNB1	catenin (cadherin-associated protein), beta 1, 88 kDa	84,106
9093	DNAJA3	DnaJ (Hsp40) homologue, subfamily A, member 3	22
2202	EFEMP1	EGF containing fibulin-like extracellular matrix protein 1	22
5610	EIF2AK2	eukaryotic translation initiation factor 2-alpha kinase 2	22
2051	EPHB6	EPH receptor B6	this study
54942	FAM206A	family with sequence similarity 206, member A	22
25827	FBXL2	F-box and leucine-rich repeat protein 2	22
2274	FHL2	four and a half LIM domains 2	22
23770	FKBP8	FK506 binding protein 8, 38 kDa	this study; [43,45]
2316	FLNA	filamin A, alpha	12
2495	FTH1	ferritin, heavy polypeptide 1	22
8880	FUBP1	far upstream element (FUSE) binding protein 1	107
2534	FYN	FYN oncogene related to SRC, FGR, YES	22
11345	GABARAPL2	GABA(A) receptor-associated protein-like 2	this study
54826	GIN1	gypsy retrotransposon integrase 1	22
2801	GOLGA2	golgin A2	22
2874	GPS2	G protein pathway suppressor 2	22
2885	GRB2	growth factor receptor-bound protein 2	22
2931	GSK3A	glycogen synthase kinase 3 alpha	22
2932	GSK3B	glycogen synthase kinase 3 beta	22
3055	HCK	hemopoietic cell kinase	22
3320	HSP90AA1	heat shock protein 90 kDa alpha (cytosolic), class A member 1	22
3303	HSPA1A	heat shock 70 kDa protein 1A	108
3315	HSPB1	heat shock 27 kDa protein 1	109
3537	IGLC1	immunoglobulin lambda constant 1 (Mcg marker)	22
79711	IPO4	importin 4	22
3843	IPO5	importin 5	22
3683	ITGAL	integrin, alpha L (antigen CD11A (p180), lymphocyte function-associated antigen 1; alpha polypeptide)	22
6453	ITSN1	intersectin 1	this study
3716	JAK1	Janus kinase 1	22

Table 1. continued

gene ID	symbol	description	refs
3932	LCK	lymphocyte-specific protein tyrosine kinase	22
55679	LIMS2	LIM and senescent cell antigen-like domains 2	22
4067	LYN	v-yes-1 Yamaguchi sarcoma viral related oncogene homologue	22
9448	MAP4K4	mitogen-activated protein kinase kinase kinase kinase 4	this study
6300	MAPK12	mitogen-activated protein kinase 12	22
4155	MBP	myelin basic protein	22
4256	MGP	matrix Gla protein	110
55233	MOB1A	MOB kinase activator 1A	22
4673	NAP1L1	nucleosome assembly protein 1-like 1	22
4674	NAP1L2	nucleosome assembly protein 1-like 2	22
10397	NDRG1	N-myc downstream regulated 1	22
4778	NFE2	nuclear factor (erythroid-derived 2), 45 kDa	22
11188	NISCH	nischarin	this study
4924	NUCB1	nucleobindin 1	22
4938	OAS1	2′-5′-oligoadenylate synthetase 1, 40/46 kDa	22
5007	OSBP	oxysterol binding protein	111
64098	PARVG	parvin, gamma	22
5170	PDPK1	3-phosphoinositide dependent protein kinase-1	22
5297	PI4KA	phosphatidylinositol 4-kinase, catalytic, alpha	22
5291	PIK3CB	phosphoinositide-3-kinase, catalytic, beta polypeptide	22
5295	PIK3R1	phosphoinositide-3-kinase, regulatory subunit 1 (alpha)	55,84,106
5300	PIN1	peptidylprolyl cis/trans isomerase, NIMA-interacting 1	112
5307	PITX1	paired-like homeodomain 1	22
5347	PLK1	polo-like kinase 1	113
10654	PMVK	phosphomevalonate kinase	22
5478	PPIA	peptidylprolyl isomerase A (cyclophilin A)	114,115
10848	PPP1R13L	protein phosphatase 1, regulatory subunit 13 like	22
5515	PPP2CA	protein phosphatase 2, catalytic subunit, alpha isozyme	116
5518	PPP2R1A	protein phosphatase 2, regulatory subunit A, alpha	116
5698	PSMB9	proteasome (prosome, macropain) subunit, beta type, 9 (large multifunctional peptidase 2)	22
5757	PTMA	prothymosin, alpha	22
5894	RAF1	v-raf-1 murine leukemia viral oncogene homologue 1	22
6142	RPL18A	ribosomal protein L18a	22
6167	RPL37	ribosomal protein L37	this study
6238	RRBP1	ribosome binding protein 1 homologue 180 kDa (dog)	22
91543	RSAD2	radical S-adenosyl methionine domain containing 2	117
6252	RTN1	reticulon 1	this study
10313	RTN3	reticulon 3	this study
6424	SFRP4	secreted frizzled-related protein 4	22
81858	SHARPIN	SHANK-associated RH domain interactor	22
64754	SMYD3	SET and MYND domain containing 3	22
8470	SORBS2	sorbin and SH3 domain containing 2	22
10174	SORBS3	sorbin and SH3 domain containing 3	22
6714	SRC	v-src sarcoma (Schmidt-Ruppin A-2) viral oncogene homologue (avian)	22
10847	SRCAP	Snf2-related CREBBP activator protein	22
6741	SSB	Sjogren syndrome antigen B (autoantigen La)	22
284297	SSC5D	scavenger receptor cysteine rich domain containing (5 domains)	110
6772	STAT1	signal transducer and activator of transcription 1	118
25777	SUN2	Sad1 and UNC84 domain containing 2	this study
6850	SYK	spleen tyrosine kinase	119
4070	TACSTD2	tumor-associated calcium signal transducer 2	22
6880	TAF9	TAF9 RNA polymerase II, TATA box binding protein (TBP)-associated factor, 32 kDa	22
6908	TBP	TATA box binding protein	22
7046	TGFBR1	transforming growth factor, beta receptor 1	22
7057	THBS1	thrombospondin 1	22
374395	TMEM179B	transmembrane protein 179B	22
7110	TMF1	TATA element modulatory factor 1	22
7157	TP53	tumor protein p53	22
7159	TP53BP2	tumor protein p53 binding protein, 2	22
7186	TRAF2	TNF receptor-associated factor 2	22
11078	TRIOBP	TRIO and F-actin binding protein	22

Table 1. continued

gene ID	symbol	description	refs
51061	TXNDC11	thioredoxin domain containing 11	22
53347	UBASH3A	ubiquitin associated and SH3 domain containing A	22
10869	USP19	ubiquitin specific peptidase 19	22
9218	VAPA	VAMP (vesicle-associated membrane protein)-associated protein A, 33 kDa	22
9217	VAPB	VAMP (vesicle-associated membrane protein)-associated protein B and C	this study; 22,28,46
10493	VAT1	vesicle amine transport protein 1 homologue (*T. californica*)	this study
55737	VPS35	vacuolar protein sorting 35 homologue (*S. cerevisiae*)	22
6293	VPS52	vacuolar protein sorting 52 homologue (*S. cerevisiae*)	22
140612	ZFP28	zinc finger protein 28 homologue (mouse)	this study
9726	ZNF646	zinc finger protein 646	22

Quantitative Reverse-Transcription PCR (qRT-PCR)

Total RNA was prepared from the cell and culture supernatant using the RNeasy mini kit (QIAGEN, Hilden, Germany) and QIAamp Viral RNA Mini Kit (QIAGEN), respectively. First-strand cDNA was synthesized using high capacity cDNA reverse transcription kit (Applied biosystems, Carlsbad, CA, USA) with random primers. Each cDNA was estimated by Platinum SYBR Green qPCR Super Mix UDG (Invitrogen) as per the manufacturer's protocol. Fluorescent signals of SYBR Green were analyzed with ABI PRISM 7000 (Applied Biosystems). The HCV internal ribosomal entry site (IRES) region and human glyceraldehyde-3-phosphate dehydrogenase (GAPDH) gene were amplified with the primer pairs 5′-GAGTGTCGTGCAGCCTCCA-3′ and 5′-CACTCG-CAAGCACCCTATCA-3′, and 5′-GAAGGTCGGAGT-CAACGGATT-3′ and 5′-GATGACAAGCTTCCCGTTCTC-3′, respectively.[42] The quantities of the HCV genome and the other host mRNAs were normalized with that of GAPDH mRNA. RTN1 and RTN3 genes were amplified using the primer pairs purchased from QIAGEN.

Cell Lines and Virus Infection

Cells from the Huh7OK1 cell line are highly permissive to HCV JFH1 strain (genotype 2a) infection compared to Huh 7.5.1 and exhibit the highest propagation efficiency for JFH1.[43] These cells were maintained at 37 °C in a humidified atmosphere and 5% CO_2, in the Dulbecco's modified Eagle's medium (DMEM) (Sigma, St. Louis, MO, USA) supplemented with nonessential amino acids (NEAA) and 10% fetal calf serum (FCS). The viral RNA of JFH1 was introduced into Huh7OK1 as described by Wakita et al.[44] The viral RNA of JFH1 derived from the plasmid pJFH1 was prepared as described by Wakita et al.[44]

Statistical Analysis

Experiments for RNAi transfection and qRT-PCR were performed two times. The estimated values were represented as the mean ± standard deviation (n = 2). The significance of differences in the means was determined by the Student's t-test.

RESULTS AND DISCUSSION

Identifying Host Proteins That Interact with HCV NS5A Protein

We employed an integrated approach that combined an experimental Y2H assay and comprehensive literature mining to identify human host proteins interacting with NS5A.

First, we performed an Y2H screening to characterize the interactions between NS5A and host proteins. The analysis of positive colonies revealed 17 host factors as interacting partners of NS5A (Tables 1, S1, Supporting Information), 14 of which are novel. The other three interactions have been characterized previously; vesicle-associated membrane protein (VAMP)-associated protein B (VAPB), a membrane trafficking factor, and FK506-binding protein 8 (FKBP8), an immunoregulation protein, independently regulate HCV replication via interactions with NS5A;[28,43,45,46] Bridging integrator 1 (BIN1), a tumor suppressor protein, interacts with NS5A and significantly contributes to HCC.[47] Among the newly discovered interactors, MAP4K4 is overexpressed in HCC, and knockdown of MAP4K4 expression inhibits HCC progression;[48] RTN1 and VAT1 were previously observed to be elevated in HCV infected cells,[49] and ARL6IP1, EPHB6, GABARAPL2, ITSN1 and NISCH were differentially expressed in HCV infection in vitro.[50] Furthermore, five (ARL6IP1, FKBP8, RTN1, RTN3, VAPB) of the 17 interactors (29.4%) localize to the endoplasmic reticulum (ER; GO:0005783; p = 0.0028), which is consistent with the role of NS5A as a crucial constituent of the HCV replication complex associated with the ER.[51] These results suggest that the PPIs detected by our Y2H assay may closely reflect NS5A interactions in vivo.

We next scanned the biomedical literature to expand the repertoire of NS5A–host interactions. Because of an ever increasing volume of biomedical literature describing the pathogenesis of infectious diseases, the identification of specific host–pathogen interactions and their roles in pathogenicity is a nontrivial task, and therefore, recent years have witnessed a rapid development of computational tools for biomedical literature mining. We performed extensive literature mining using computational tools that facilitate the retrieval and extraction of relevant information from the biomedical literature (Pubmed, EBIMed, Protein Coral) and followed it up with a careful manual inspection to identify additional host factors, which directly interact with NS5A and which were not present in the Y2H data set. One hundred and fifteen pairwise interactions between NS5A and human proteins (consisting of 93 catalogued by a high throughput study of binary HCV–host interactions[22] and 22 from assorted reports; see Supporting Information, Table S2) were extracted from the literature in this manner and were added to the existing interactors. The resulting NS5A–human interactome thus comprised 132 human host proteins directly interacting with NS5A (Table 1), all of which are expressed in the liver (see Supporting Information, Table S3).

Network Topological Analysis of the NS5A–host Interactions: NS5A Preferentially Targets Hubs and Bottlenecks in the Host Protein Interactome

To further understand the biological significance of the NS5A–host interactions, we retrieved PPIs for the nodes targeted by

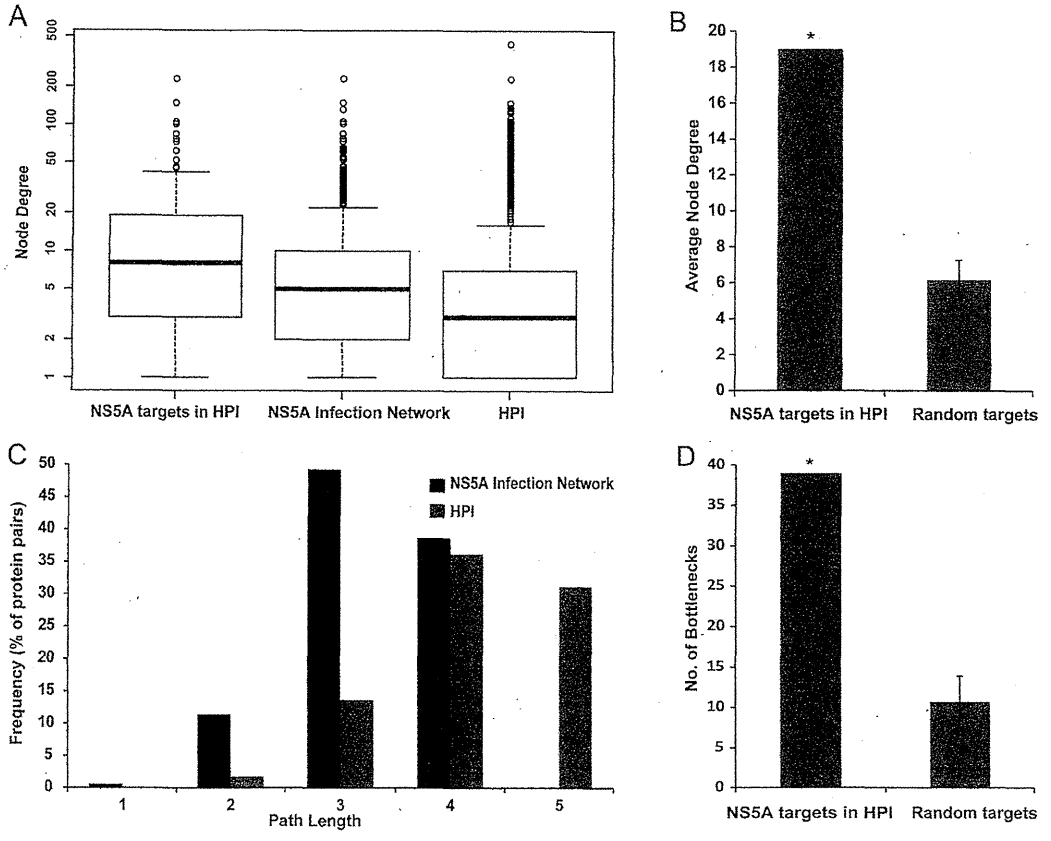

Figure 1. Topological analysis of the NS5A infection network. (A) The node degree distributions of the NS5A interatcors in the HPI, NS5A infection network, and HPI are represented as box plots. The average degree of the NS5A interactors in HPI (19.02) was higher than those of the NS5A infection network (8.24) and HPI (5.96). Median node degrees (indicated by thick horizontal lines) of the NS5A interactors in HPI, NS5A infection network, and HPI are 8, 5, and 3, respectively. (B) The average degree of the nodes targeted by NS5A in HPI was much higher than mean average degree of 1000 sets of the randomly selected 108 nodes in HPI. (C) The shortest path length distributions of the NS5A infection network and HPI. The path length is represented on the x-axis while the y-axis describes the frequency, i.e., the percentage of node (protein) pairs within the PPI network with a given shortest path length. For simplicity, only the node frequencies for path lengths 1−5 in the HPI are displayed. (D) The number of bottlenecks among the nodes targeted by NS5A in HPI was much higher than mean of the number of bottlenecks among 1000 sets of the randomly selected 108 nodes in HPI. *: $p < 0.001$.

NS5A in the HPI and incorporated them with the initial interactions to infer an extended NS5A infection network. PPIs for 108 of 132 NS5A interactors were retrieved in this manner; 24 of 132 NS5A interactors had no PPIs in the HPI (Supporting Information, Tables S4, S5a, S5b). For the NS5A infection network and the HPI, we computed the node degree distribution and the characteristic/average path length measures to capture the topologies of the two networks. The degree of a protein, which corresponds to the number of its interacting partners, may often reflect its biological relevance since a better connected protein is likely to have a higher ability to influence biological networks via PPIs. Average path lengths provide an approximate measure of the relative ease and speed of dissemination of information between the proteins in a network.

The NS5A infection network consisted of 1442 entities (nearly all of which are expressed in the liver; see Supporting Information) with 6263 interactions between them (Supporting Information, Tables S4, S5a). The average degree (defined as the number of interactions for a given protein) of the NS5A infection network (8.24) was notably higher than the degree inferred for the HPI (5.96) (Figure 1A). Furthermore, the average degree of the nodes targeted by NS5A in the HPI (19.02) was even higher; this number is significantly greater than the average degree obtained from a sample of randomly selected nodes (6.17 ± 1.08 with $p < 0.001$; Figure 1B; see Supporting Information). Also the degrees inferred for the majority of the NS5A interactors in the HPI (65 of 108; 60.18%) were higher than the mean degree of the HPI (5.96) (Figure 1A). Our observations therefore suggest that NS5A preferentially targets several highly connected cellular proteins (hubs) with an ability to influence a large number of host factors in HCV infection. The average (shortest) path length of the NS5A infection network (3.26) was significantly shorter than the HPI (4.54), and also the distribution of shortest path lengths was shifted toward the left (Figure 1C), thereby suggesting that the NS5A influenced cellular network is more compact and inclined toward faster communication between the constituents relative to the host cellular network.

Next, we examined the betweenness measures of the NS5A interactors in the HPI to assess their significance in the HPI and the NS5A infection network. The betweenness of a node, determined by the number of shortest paths passing through it, reflects the importance of that node in the network; the nodes

with the highest betweenness prominently regulate the flow of signaling information and are therefore "bottlenecks", representing central points for communication in an interaction network.[52] Previously, proteins with high betweenness have been implicated in crucial roles in HCV infection and pathogenesis.[53,54] To investigate if NS5A preferentially targets bottlenecks (defined as the top 10% of the nodes in the HPI ranked by betweenness), we estimated the fraction of NS5A interactors that were bottlenecks in the HPI. A significant proportion (39 of 108; 36.1%) of the NS5A interactors were identified as bottlenecks in the HPI (Supporting Information, Table S6); this number is significantly higher than the number of bottlenecks among randomly selected nodes (10.72 ± 3.17 with $p < 0.001$; Figure 1D; see Supporting Information). These include growth factor receptor-binding protein 2 (GRB2), which plays an important role in the subversion of host signaling pathways by NS5A;[55] tumor protein 53 (TP53), a key mediator of the oncogenic effect of NS5A in HCV-induced HCC;[56] and tyrosine kinase SRC, which regulates the formation of NS5A-containing HCV replication complex.[57] Among the NS5A interacting proteins identified by our Y2H screening, ITSN1, an endocytic traffic associated protein, and GABARAPL2, an autophagy associated protein, were identified as network bottlenecks.

Our observations therefore suggest that NS5A preferentially interacts with highly central proteins in the host protein interactome; these interactions may help the virus to regulate efficiently the flow of the infection-related information in the host cellular network and manipulate the host metabolic machinery for its own survival and pathogenesis. Our observations are consistent with studies that suggested that viral pathogens tend to interact with well-connected host proteins that are central to the host cellular networks, thus enabling them to appropriate essential cellular functions.[21,22,26,58,59]

Functional Analysis of NS5A Interaction Network

Next, we investigated the NS5A infection network for the enrichment of specific biological associations (KEGG pathways, CATH structural domains; GO terms and Reactome Pathways; Supporting Information, Tables S7a, S7b, S7c and S7d). Notably, a significant proportion of the proteins in the NS5A infection network were mapped to the CATH Phosphorylase Kinase; domain 1, domain (CATH:3.30.200.20; 138 out of 1442, $p = 2.61 \times 10^{-45}$) including 23 of the 132 NS5A interacting host proteins ($p = 3.38 \times 10^{-14}$) (13 of which are bottlenecks in the HPI), based on the Gene3D protein domain assignments (Supporting Information, Table S7b). These include two novel interactions between EPHB6 (a kinase deficient receptor) and MAP4K4 and NS5A, identified by our Y2H assay (Table 1). The significant representation of cellular kinases in the NS5A infection network is consistent with the key roles played by reversible phosphorylation of NS5A in modulating various NS5A functions in HCV pathogenesis. Impairing NS5A hyperphosphorylation has been shown to inhibit HCV replication, and thus, the cellular kinases that regulate NS5A phosphorylation are important targets for anti-HCV therapy.[9,60−63]

The analysis of NS5A infection network revealed an enrichment of 79 KEGG pathways (Supporting Information, Table S7a). Furthermore, 31 of the 39 NS5A interacting bottlenecks (hereafter referred to as bottlenecks) were mapped to 75 of the 79 enriched KEGG pathways (Supporting Information, Table S5). Among the 75 bottleneck-associated enriched KEGG pathways, the highest numbers were associated with various cancers and infectious diseases (31 enriched KEGG pathways; 27 bottlenecks), followed by immune system, signal transduction and endocrine system (23 enriched KEGG pathways; 27 bottlenecks), cell growth and death (4 enriched KEGG pathways; 9 bottlenecks), nervous system (4 enriched KEGG pathways; 8 bottlenecks) and cellular communication (3 enriched KEGG pathways; 14 bottlenecks) among others (Tables 2, S8a, Supporting Information). Below we describe our observations on the most prominent enriched biological themes of interest that were associated with the NS5A infection network, with a specific focus on the bottlenecks.

Cancers and Infectious Diseases

The analysis of the NS5A interaction network revealed that NS5A specifically targets host factors that participate in various complex human diseases. Thirty-four NS5A interactors including 24 bottlenecks were mapped to one or more of the 17 enriched KEGG pathways associated with different infectious diseases (Supporting Information, Tables S7a, S8a). Among the most prominent associations, 12 bottlenecks were mapped to "Epstein–Barr virus infection" ($p = 1.36 \times 10^{-27}$); 10 to "Hepatitis C" ($p = 3.47 \times 10^{-24}$); 10 to "HTLV-I infection" ($p = 1.39 \times 10^{-20}$); 9 to "Hepatitis B" ($p = 3.33 \times 10^{-26}$); 8 to "Measles" ($p = 5.69 \times 10^{-17}$); 7 bottlenecks were mapped to "Influenza A" ($p = 5.01 \times 10^{-12}$); 7 to "Herpes simplex infection" ($p = 1.47 \times 10^{-13}$) and 6 to "Tuberculosis" ($p = 3.02 \times 10^{-6}$) (Supporting Information, Tables S7a, S8a). These associations include infectious diseases induced by various bacterial and viral pathogens thereby suggesting that HCV and other pathogens may systematically target specific host factors, the perturbation of which may contribute to the onset of various human diseases.

Also, 19 bottlenecks were mapped to one or more of the 16 enriched KEGG pathways associated with various cancers. Among the most prominent associations, 10 bottlenecks were mapped to "Viral carcinogenesis" ($p = 1.3 \times 10^{-30}$); 8 each were mapped to "Prostrate cancer" ($p = 4.27 \times 10^{-25}$), "Endometrial cancer" ($p = 5.52 \times 10^{-21}$) and "Colorectal cancer" ($p = 4.22 \times 10^{-18}$); 7 to "Pancreatic cancer" ($p = 1.94 \times 10^{-18}$); 6 to "Chronic myeloid leukemia" ($p = 1.61 \times 10^{-30}$) and 5 each to "Non-small cell lung cancer" ($p = 8.66 \times 10^{-15}$) and "Glioma" ($p = 2.38 \times 10^{-14}$) (Supporting Information, Tables S7a, S8a). The significant association of HCV with host factors central to various cancer pathways (including tumor suppressors such as TP53) is consistent with previous observations that viral pathogens significantly targeted host proteins associated with cancer pathways,[59,64,65] which likely plays major roles in tumorigenesis.

Immune System and Signal Transduction

HCV infection induces various active and passive host immune responses including the recognition of viral RNA by host cell receptors. These events lead to the production of Type I interferons (IFN-α/β) and inflammatory cytokines in the infected hepatocytes, initiating the antiviral response. HCV persistence in the host is determined by the virus's ability to impair host immune responses.[66−69]

The analysis of the NS5A interaction network revealed that 21 of the 132 NS5A interacting proteins, including 16 bottlenecks and their interacting partners, were mapped to one or more enriched KEGG pathways associated with the immune system (Supporting Information, Tables S7a, S8a).

dx.doi.org/10.1021/pr3011217 | J. Proteome Res. 2013, 12, 2537−2551